Evaluation of αLphav Integrin Role in Mouse Model Induced Periapical Periodontitis

Forsyth
Pioneering Discoveries
Profound Change

Evaluation of αlphav integrin role in mouse model induced periapical periodontitis

A Thesis presented by:

Ziyad Allahem, BDS, MS

To

The Faculty of Medicine at Harvard University

In partial fulfillment of the requirements for the Degree of

Doctorate of Medical Sciences

Research Mentor:

Susan Rittling, PhD

The Forsyth Institute

Harvard School of Dental Medicine

March 2016

Acknowledgement

I would like to express my deepest gratitude to my mentor, Dr. Susan Rittling. Her incomparable passion and devotion truly inspired me on this project. Her motivation, bounty and endurance have made it possible for me to endure this research project through its tough times.

I feel tremendously treasured to have been a part of the immunology department at the Forsyth institute. This research would not have been possible without the support, work and friendship of the members of the immunology department. I thank Dr. Hajime Sasaki for his knowledge, help and patience. I'm appreciative for all the members of the Forsyth Institute for providing me with a fruitful research environment which brought this project to life, specially Tommy Hui, Rani Singh, Chris Johnson and Montse Ruiz Torruella who worked with me in Dr. Rittling lab.

I would like to thank the members of my thesis committee Dr. Toshihisa Kawai, Dr. Yefu Li and Dr. Tatiana Besschetnova whom played a key role in the completion of this work. Their valuable remarks, ideas and recommendations significantly improved this project.

I would like to extend my gratitude to Dr. Robert White and Dr. Tom Pagonis for their unmatched support, time and effort. Their guidance has significantly influenced the quality of this project.

TABLE OF CONTENTS

Figures and Tables

Abstract:

Background: alphav (av) integrin is the most common integrin alpha subunit, it is expressed in different cells and involved in many cellular process including adhesion, migration, survival and growth factor signaling. alphav on immune cells has a role in promoting T regulatory (Treg) cells production and differentiation of T helper 17 (Th17) through activating TGF-beta as shown in conditional knockout of alphav in immune cells. Osteopontin (OPN) is a ligand for alphav and involved in modulation of inflammation through its interaction with alphav in immune cells. OPN has been shown to have a protective role in endodontic infection, so we predict alphav to have similar role. The aim of the study is to establish the role of αv integrin in the immune response to endodontic polymicrobial infection, using an established mouse model of endodontic infection

Methods: alphav$^{fl/fl}$ mice were mated with mice expressing Cre under the control of the Tie2 promoter, which is expressed in all cells of the hematopoietic lineage as well as in endothelial cells. These mice were subjected to pulp exposure and infection with a mixture of four endodontic pathogens. Bone loss was assessed 0, 7, 14, and 21 days after infection using micro CT. Inflammation and neutrophils enumeration in periapical area evaluated using immunohistochemistry, also osteoclast presence in periapical area examined with TRAP staining. Microarray and qPCR used to investigate cellular and

cytokines activity changes. Blood plasma collected from mice during sacrificing was evaluated using ELISA for level of IgG's and antibody activity against the specific bacteria used for the infection.

Results: Lack of alphav expression was confirmed on neutrophils by FACS. Twenty-one days after pulp exposure and infection with oral pathogens, 6 of 16 av-tie2cre KO mice developed swelling and abscesses in the mandible, while no abscesses were observed in control mice. However, the periapical bone resorption was similar in the two groups. Strikingly, ectopic bone formation on the buccal and lingual aspects of the mandibular surface was observed only in the av-tie2cre animals, suggesting a severe disruption of bone turnover caused by the inflammatory process in these animals. Neutrophils showed decrease in number in periapical area and microarray and the observe disseminating infection suggested a B cells defect either in function or migration.

Conclusions: Together, these results demonstrate a critical role for the alphav integrin in the suppression of inflammation during the process of endodontic infection.

Introduction:

Periapical periodontitis is an endodontic infection that results from oral bacteria invading the dental pulp (1, 2). As carious lesions become extensive or when tooth cracks or fractures expose the pulp, endogenous oral bacteria advance to the pulp chamber, where inflammation develops. If the lesion is not removed, the pulp will degrade and the bacteria will infect the pulp resulting in complete necrosis of the pulp complex, leading to inflammation of the periapical tissue which is called periapical periodontitis. These lesions have different classifications depending on the clinical signs and symptoms of the patient (3). Failure of the host response to eradicate these infections results in an intense inflammatory response, leading to tissue destruction and bone degradation (4).

Endodontic infection occurs as the bacteria colonize the necrotic dental pulp. The bacteria present vary from individual to individual, and consist of a mixture of 10-30 different anaerobic species (5). Although Gram-negative species, such as *Fusobacterium nucleatum, Prevotella intermedia, Prevotella nigrescens*, Porphyromonas endodontalis, are most commonly reported in association with these infections, Gram-positive species are also found in abundance in the root canal infections for example, *Parvimonas micra, Streptococcus anginosus, Streptococcus mitis,* and *Streptococcus sanguinis* (5-7).

Dental Pulp immune system

Dental pulp tissue contains a network of immunocompetent cells including class II antigen presenting dendritic cells (DC) in the odontoblast layer; and macrophages, neutrophils, and T lymphocyte in the center of the pulp; while B cell are undetectable (8, 9). The initial response to the invading bacteria is the innate immune system through influx of polymorphonuclear cells (PMN) (10, 11). The cellular involvement increases to include T and B cells after dendritic and macrophages recognize the bacteria antigens and process them to adaptive immune cells present locally or through recruitment from regional lymph nodes.

Periapical lesion development

Inflammation of periapical tissue starts as early as 3 days from bacteria invading the pulp and before complete necrosis of the pulp (12), and includes influx of PMNs and monocyte (13). The periapical response could be considered as an immune response to enclose and contain the infection (14) and has similar cellular features to pulp infection. Cellular infiltrate includes macrophages, PMN, T-lymphocyte, B-lymphocytes, eosinophil, mast cells, natural killer and plasma cells (13, 15-17). Non-inflammatory cells are also represented in periapical lesions including fibroblasts, osteoblasts, osteoclasts, proliferating epithelium and vascular endothelium (18, 19).

Rodent models have been established and used to replicate the human periapical infection and helped to study the kinetics of the cellular response and

the immunopathology of the inflammatory periapical lesion (1, 19). Different laboratories have used these rat and mouse models by surgically inducing pulp exposure in the animal molar teeth to mimic pulpal and periapical infection. Pulpal necrosis will start in day 2 followed by severe destruction of bone in the periapical area between days 7 and 20 (active phase) then bone resorption will stabilize (chronic phase) (13, 17, 19).

Bone resorption in periapical periodontitis

Bone resorption in periapical periodontitis can be regarded as a host defense mechanism to limit the infection and the bacteria to pulp canals (14). In early work a study of human periapical lesions tissue extracted during periapical surgery to evaluate bone resorption activity, revealed that the activity of bone resorption was mainly due to cytokines activity rather than bacteria lipopolysaccharide (LPS). The study showed treating the tissue with polymyxin B, an antibiotic that neutralizes LPS, or heat treatment did not stop the activity, while higher temperature (70C) or treatment with proteinase K could neutralize the activity indicating that bone resorption activity source is a protein (20). Also, the study showed using anti-interlukin-1a (IL-1a), and anti-tumor necrosis factor-B (TNF-b) known now as lymphotoxin reduced the majority of the activity. In a rat model, periapical lesions bone resorption activity was found to correlate with increased expression of RANKL early in the lesion development indicating a role of RANKL in osteoclast differentiation. Also, the researchers in this study observed up regulation of IL-1a, IL-1b, and TNF-a cytokines which promote

osteoclast function and formation, suggesting a synergistic effect between them and RANKL (21). Interleukin-6 (IL-6) is an immune modulator and a pro-inflammatory cytokine. It is produced locally in the bone through stimulation of IL-1 and TNF (22). In a study of IL-6 knockout (KO) mice the periapical lesion size increased in KO mice compared with WT with increased osteoclast numbers and IL-1 cytokine level which indicating an anti-inflammatory role for IL-6 and negative feed back to IL-1 in periapical area (22) .

In another study where mice lack effective Toll-like receptors (TLRs) 4, periapical bone destruction was lower compared with wild type and was correlated with lower expression of bone resorptive cytokines IL-1a and b cytokines (23). They concluded in this study that the decreased expression of the cytokines was a direct effect of TLR-4 rather than an indirect effect mediated by Th-1,2 cells cytokines modulation.

Cellular Infiltrate and role in periapical lesion

Both innate and adaptive immune response involved in periapical periodontitis, although the innate immunity is the first line of defense to the invading bacteria and its by-products (24). This is demonstrated by genetic abnormalities resulting in increased susceptibility to infections such as periodontitis. Individual with different polymorphonuclear leukocyte (PMNs) function disorders like Papillion-lefevre syndrome, leukocyte adhesion deficiencies (LAD), cystic neutropenia and others exhibit increase incidence and severity of periodontal disease (25, 26). Also, LAD patients show early onset

periodontitis (27, 28). There are two types of LAD, LAD-I due to beta-2 integrin mutation, while LAD-II due to defect in fucosylation of ligands for selectins. Both types develop severe infection due to inability of PMNs to migrate to infection tissue and leukocytosis which make this disease a good model to study the role of PMNs in periapical lesions in animals. In genetically modified knockout mice lacking P-selectins and E-selectins, mimicking LAD-II condition, the mice exhibit bigger periapical lesion destruction associated with less PMNs number in the lesion and increased IL-1a (29). In this knockout the endothelium lacked expression of P- and E-selectins which are important in neutrophil extravsation stimulated by LPS and TNF-a. Together, these finding show the importance of PMNs in the control of endodontic infections.

The role of neutrophils in periapical lesion has been studied. In wild type mice, after pulp exposure the animals were injected with cyclophosphamide, which induces neutropenia. The results showed a lack of PMNs in the periapical lesion, increased periapical bone destruction, and bacteria were isolated from the pulp and periapical tissue (30). In a second study, however, induction of neutropenia in infected mice with methotrexate, resulted in smaller periapical lesion formation (31). This difference can be related to the agent used as since they may modulate the lymphocyte functions too. In an effort to study the role of PMNs, a rat study used the immune response modifier PGG-glucan (soluble poly- beta1 -6-glucotriosyl-beta1 -3-glucopyranose glucan), which increases host response against bacteria without pro-inflammatory mediators. Administration of PGG-glucan resulted in decreased periapical lesion with less percentage of pulp

necrosis. These results can be explained by increased number of circulating neutrophils in the blood and improved phagocytic activity of the neutrophils (32).

Both T-helper (TH) and T-suppressor (TS) cells have been found in the periapical lesions with reduced ratio of TH/TS to about 1 compared to around 2 in the blood (17, 33) similar to results found in deep periodontal pocket (34). Immunoglobulin-producing cells have been identified in the periapical lesions with IgG positive cells the most abundant, around 70%, followed by IgA, IgE, and IgM (15, 35, 36). In a rat study, lymphocytes were found to be the most common cells in the periapical lesion followed by PMNs and monocyte-macrophages and the distribution of the cells did not differ between different time points (19, 37).

In an approach by Stashenko et. al. to study the role of T- and B-cells in endodontic infection, RAG-2 severe combined immunodeficient (SCID) knockout mice were used (38). These mice have immature B and T cells functions, which lack specific antibody and cell-mediated responses. One third of the mice developed orofacial swelling, abscess and increased periapical lesion area, accompanied by weight loss in response to endodontic infection. The orofacial swelling and weight loss indicate disseminating infection and sepsis. Further the same lab repeated the study with Igh-6 (B-cell-deficient), Tcrb Tcrd (T-cell-deficient) mice models to investigate which of these cells were involved more in preventing infection dissemination and sepsis. First, they repeated the RAG-2 SCID experiment with modification of the infection protocol, where the exposed tooth been sealed after the exposure and inoculation of the bacteria in order to prevent communication with the oral cavity and drainage of the abscess which

may resemble most of the pulp infection in human. The percentage of the RAG-2 SCID mice with orofacial abscess increased to 80-90% due to sealing of the teeth. B-cell deficient mice developed a similar phenotype, where 50% of the mice showed abscess and weight loss. Furthermore, passive transferred of specific antibody against infecting bacteria suppressed the phenotype in the B-cell deficient mice. On the other hand, none of the T-cell deficient mice showed dissemination signs, abscess or weight loss (39). These results suggest B cell role in suppressing and controlling periapical lesion and preventing spread of infection and septicemia.

Role of IL-17 in periapical lesion

IL-17 is considered mostly as a pro-inflammatory cytokine produced mainly by Th17 cells, γδ T cells, neutrophils and macrophages (40). A study has been performed using IL-17 receptor A (IL-17RA) knockout mice, in which the major receptor for IL-17A and F, immunoregulatory ligands from the IL-17 family, is deleted, to investigate its role in endodontic infection. The study concluded a protective role for IL-17 in periapical periodontitis (41), as they showed periapical lesion size increased in IL-17RA KO compared to WT and in WT mice when IL-17 was neutralized with antibody. They showed that at 21 days post infection the inflammation was persistent and acute in IL-17 RA KO mice with profound infiltration of neutrophils, macrophages and elevated level of IL-1a, IL-1b and macrophage inflammatory protein 2 (MIP-2) which is a potent chemoattractant for neutrophils (42).

Role of Osteopontin (OPN) in periapical lesion and inflammation

Osteopontin (OPN), one of the alphav integrin ligands, enhances the immune response during inflammation by promoting chemotaxis to the site of injury and acts as an adhesion molecule to bind the inflammatory cells to the injured site (43, 44). Also, it may promote inflammation by stimulating pro-inflammatory cytokines (45). In a study to determine the role of OPN in endodontic infection showed OPN knockout mice developed a bigger periapical lesion size and more inflammation area compared to WT (46). The increased inflammation and bone resorption in OPN knockout was associated with increased expression of bone resorption related cytokines IL-1a and RANKL. The study showed OPN plays a protective role in endodontic infection. In another OPN knockout mice studies, the immune system was deteriorated in response to injury and infection (47). Also, neutrophils showed less peritoneal recruitment due to a possible defect in chemotactic and chemokinetic migration mechanisms, resulting from a lack of endogenous OPN (48). Although OPN is known to have a pro-inflammatory function, it also works to regulate hyper-inflammation as in LPS induced endotoxeima where secretory OPN produced by spleen macrophages has shown to induce T cell (CD4+) migration through interaction with alphav integrin to the spleen to interact with macrophages and lead to down regulation of TNF cytokines expression and control of hyper-inflammation (49). OPN has a significant role in inflammation and we expect this role to diminish in mice lacking alphav integrin, which has a high affinity ligand for alphav integrin (50).

alphav integrin role in immune response

Integrins are a family of cell adhesion receptors that facilitate cell-cell and cell-extracellular matrix signaling and communication**.** They consist of heterodimers of alpha and beta subunits with different sets of combination. There are 18 alpha and 9 beta subunits that make up around 24 integrins. They respond to extracellular signaling, outside-in, which regulate cell differentiation, motility, migration and survival (51, 52). In addition, the cell can induce conformation changes in the integrin which alters affinity to outside molecules, so-called inside-out activation (53). Integrins bind to certain ligands through recognizing a specific amino acid sequence such as RGD present in osteopontin, and fibronectin (54). Integrins and their ligands have an important role in development, immune response, leukocyte signaling, hemostasis and they are receptors for different bacteria and viruses (51). Also, they have been targeted for different therapeutic drugs.

alphav (α v) is the most common alpha subunit making combinations with a total of five beta subunits (beta 1,3,5,6,8). alphav is involved in many cellular process including adhesion, migration, survival and growth factor signaling**.** The majority of the alphav heterodimers recognize the RGD sequence in protein ligands including osteopontin, fibronectin, bone sialoprotien, vitronectin, thrombospondin, fibringen, von Willebrand factor, tenascin, argin and for αvβ8 laminin and type IV collagen (55-58). alphav integrin is expressed in different

cells and is essential for development as alphav knockout mice die at midgestation or immediately after birth from placental deficiencies and hemorrhage (55, 56). αvβ6 and αvβ8 are expressed in epithelium where they have a role in activating TGF-β (59), also αvβ8 is expressed in myeloid cell (60). αvβ3 and αvβ5 are up regulated during tissue injury and they are expressed in different immune cells. Their roles include cell adhesion, migration, survival, (61-63) and these integrins also have a role in phagocytosis of apoptotic cells, an important process for healing state (64).

Studies in alphav knockout have been performed using a conditional knockout technique. Tie2 is a promoter that is specifically activated in endothelial and hematopoietic cells. αv-tie2cre mice (αv KO in endothelial and hematopoietic cells) are born and develop normally up to 12 week when they start developing colitis and loss of weight (56). Lacy-Hulbert et al. and others (60) performed a series of experiments where they showed that the development of colitis was due to loss of αlphav in myeloid cells and not the adaptive T or B immune cells. Also, they showed the intestinal damage is related to two distinct roles of αlphav, defective dendritic cell (DC) function in promoting Treg cell production through its ability to activate TGF-β through avb8; and impaired function of macrophages and dendritic cells in phagocytosis of epithelial apoptotic cells through avb3, and avb5, which provide self antigen. DC failure to phagocytose epithelial apoptotic cells lead to T cells stimulation and increased the extent of the inflammation, while DC bearing apoptotic cell (functionally immature) induced Treg

differentiation and controlled inflammation (56). In a similar mechanism alphav on DC activates latent TGF- β leading to differentiation of T-cells to Th-17, as the mice lacking alphav on DC does not have the pathogenic causative Th-17 in experimental autoimmune encephalomyelitis (EAE) and accordingly does not develop the disease compared to wild type according to a study by Lacy-Hulbert et al. (65).

Transforming growth factor β (TGF-β) family consists of three isoforms (TGF-β1, -2, -3). TGF- β acts almost on all cell types with several effects including modulation of inflammatory cell function, cell proliferation and extracellular matrix production (59, 66). TGF- β is secreted as an inactive high molecular weight protein that consists of two peptides: active TGF- β, which is covalently bound to latency-associated peptide (LAP), known as small latent TGF- β. Although most cells secrete a more complex molecule of a higher molecular weight, as in addition to the small latent peptide an additional protein, latent TGF- β binding proteins (LTBPs), bind to LAP through disulfide bonds, referred to as large latent complex (67). Latency-associated peptide (LAP), one of the three proteins, is a ligand for αvβ6 integrin through its RGD sequence and leads to TGF- β activation. This could explain why mice lacking αvβ6 have excessive inflammatory response, because they lack active TGF- β (59). αlphav integrins on DCs are an essential component in the activation mechanism for latent TGF-β. Active TGF- β has a regulatory mechanism function in the immune response through its signaling for T cell differentiation to Treg and Th17 (65). Also, TGF- β

is involved in soft tissue and bone remodeling and formation through promoting periosteal mesenchymal cell differentiation into chondrocyte and osteoblast and stimulating these cells to form cartilage and bone matrix (68). The presence TGF- β was reported in the periapical area after endodontic infection but the role of this molecule has not been studied (69, 70).

Specific Aim

The purpose of this study is to understand and evaluate, for the first time, the role of alphav integrin in pathological inflammatory response induced in periapical periodontitis. alphav integrin plays a role in immune system response through modulation of immune cells migration, function, differentiation and stimulation via interaction with its different ligands. OPN is a ligand for alphav and it has been shown to play protective role in endodontic infection, so we predict alphav to have a similar affect in this disease. American Association of Endodontics estimates more than15 million endodontic procedures are performed yearly in the United States, which cost billions of dollars. Success rate for conventional root canal treatment is around 85% (71), and have not been improved much in the last few decades despite the improvement in the chemical and mechanical techniques for bacterial clearance in endodontic procedures, suggesting the need for biological means to help treat the disease. Also, endodontic infection has similar features to numerous infections in the human body, including periodontitis and soft tissue infection, which make it a good model to study. Therefore, gained knowledge from this model can be used to understand and develop therapeutic methods for other diseases (72, 73).

In our experiments we used a mouse model of induced periapical periodontitis that reproduces human endodontic infection (22, 74) to study the role of alphav in endodontic infection. We used conditional knockout mice alphav$^{-/flox}$ as complete alphav knockout mice die at or shortly after birth, to study the role of alphav in immune cells specifically in endodontic infection. Also, we explored the function

and migration of specific immune cells like neutrophils and B cells using air pouch model, immunohistochemistry and ELISA.

Hypothesis

The αlphav integrin enhances myeloid cell migration and functions, which modify the innate and adaptive immune response.

Materials and Methods:

Animals

αv$^{+/-}$, Tie2Cre+ and αv $^{flox/flox}$ mice were generously provided by Dr. Lacy-Hulbert. All mice were on a C57BL/6 background, 6-9 week-old, male and female (body weight 15-25 grams) were used for the experiments. The Tie2 promoter is active only in hematopoietic and endothelial cells, so expression of the Cre recombinase under the control of Tie2 promoter results in deletion of the floxed alleles in hematopoietic and endothelial cells (75). We generated mice lacking αlphav in hematopoietic and endothelial cells by first mating αlphav KO heterozygous (αv $^{+/-}$) with Tie2Cre transgenic mice $^{+/+}$ to create αv $^{+/-}$ Tie2Cre $^{+/+}$ (homozygous) mice. Then, we crossed those mice (av$^{+/-}$ Tie2cre$^{+/+}$) with αv $^{flox/flox}$ mice which resulted in deletion of the second alphav allele only in the cell carried the tie2 promoter, hematopoietic and endothelial, lead to generate αv–tie2 (αv $^{flox/-}$, tie2cre+) and the littermate as control mice (αv $^{flox/+}$, tie2cre+). We have used av$^{-/flox}$ mice rather than av$^{flox/flox}$ for the following reasons: the combined KO/ flox allele gives more efficient deletion as only one copy needs to be deleted, also it allows us to maximize use of littermates, which is really essential for any experiments where microbiota may be affecting phenotype. Another reason is cre line might delete in the germline, as it hard when using these line to control for this unless we keep the cre and lox alleles separate until the experimental strain. Finally, accurately genotyping them for germline versus tissue deletion is really hard. These mice were born and developed normally up to 12 week when they

start developing mild colitis and loss of weight. All mice were maintained in Forsyth Institute Animal Facility, in ventilated cages with automatic watering and ad lib access to food under a 6AM to 6PM light cycle and under specific pathogen free environment. The Forsyth's Institutional Animal Care and Use Committee (IACUC) approved all experimental protocols.

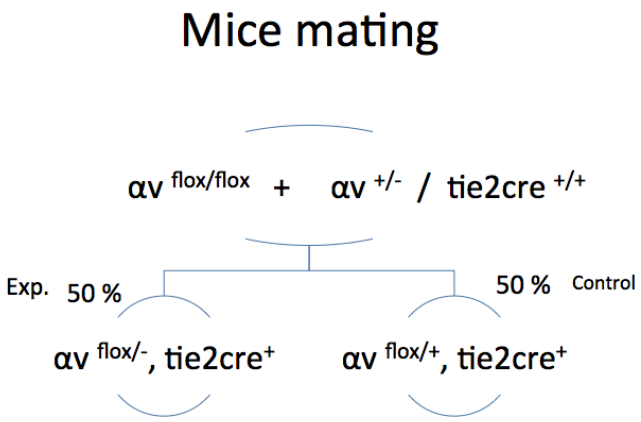

Figure 1. Mice mating strategy. Experimental mice have one knockout allele and one floxed allele, while littermates used as control have one WT and one floxed allele.

Genotype was confirmed using PCR for ear tissue and run on 1-2% agarose electrophoresis gel. In case of Tie2Cre some samples were sent to Transnetyx company (Cordova, TN) for preliminary identification of Tie2Cre homozygosity.

Primers used for mice genotype:

alphav flox :

1f: GGTGACTCAATCTGTGACCTTCAGC

rev: CACAAATCAAGGATGACCAAACTGAG

2f: TTCAGGACGGCACAAAGACCGTTG

primers 1f with rev will generate 550 base pair (bp) in wild-type mice, 700 bp in floxed mice, and 150 bp after floxed deleted using Cre. Using 2f and reverse will

give 250 in wild type and 400 bp in floxed mice and no bands in floxed deleted with Cre.

Tie2Cre:

5‘-CGCATAACCAGTGAAACAGCATTGC-3’ in Cre coding region

5‘-CCCTGTGCTCAGACAGAAATGAGA-3’ in the Tie2 promoter region, will give 450 bp band

alphav knockout:

forward: 5′-GAC GCC TTC AAC CTG GAC-3′

reverse: 5′-CTG GAT GCT GAG TGT CAG GT-3′

neoR forward: 5′-AGG ACA TAG CGT TGG CTA CC-3′

wild type will give 291 bp band and targeted allele will give 890 bp band.

Or:

forward: 5′- TCG AAA GTC CCG AGT AT-3′

Reverse: 5′-GGC CAA GTG AAG CAA GTT ACG-3′

neoR forward: 5′-GGC CGC TTT TCT GGA TTC ATC G-3′

Bacteria preparation

Prevotella intermedia ATCC 25611, *Fusobacterium nucleatum* ATCC 25586, *Streptococcus intermedius* ATCC 27335, and *Parvimonas micra* ATCC 33270 were grown on Trypticase Soy Agar with 5% sheep blood under anaerobic conditions (85% N2, 5% H2, and 10% CO2). The bacteria were harvested and suspended in 1x sterile PBS. Using spectrophotometry OD 600 =1 (equivalent of $1*10^9$ cells in 1ml) of each species were collected and mixed in one tube,

centrifuged at 3,500 rpm/min for 5 minutes and re-suspended in 20ul of 1x PBS and 20 ul of 2% carboxymethyl cellulose to increase viscosity and make it easier to inject and stay in the tooth. At the time of infection mice were injected with total of 2.5ul/tooth bacteria suspension equal $2.5*10^8$ cells/tooth using micropipette directly into the exposed tooth pulp (see below), which result in reproducible infection (46).

Pulp exposure and periapical lesion induction

Mice bodyweight were measured prior to use in the well-described mouse model that reproduces the human endodontic infection (22, 74). In this model the mouse were anesthetized by the intraperitoneal (IP) injection of Ketamine HCl (80 mg/kg of body weight) and Xylazine (10 mg/kg) in sterile phosphate-buffered saline (PBS). Anesthetized mice were mounted on a jaw retraction board for better visibility and stability, and the operation was carried out under a surgical microscope, where right and left first molars dental pulp were exposed to oral cavity using an electrical dental straight hand piece with sterilized ¼ surgical carbide round bur (SSwhite, Lakewood, NJ) until the pulp chamber is visible. Both canals orifice were probed with endodontic file no. 6 (tip size is 0.06 mm) to confirm the exposure. In addition to the mouse's normal oral flora bacteria, the mixture of four common human endodontic pathogens, as described above, are introduced in the pulp chamber to cause pulp tissue necrosis and endodontic infection, which will lead to periapical periodontitis lesion. Mice were given IP

Buprenex analgesic injection for the day of the procedure and two days after for pain management (0.01 mg/kg).

Tissue sample preparation

Mice were sacrificed (n=10/group) at 0,7,14,21 days after infection using CO2 euthanasia chamber. 0 day was defined as a control group. After the mice were sacrificed the mandible was collected, blood was collected from the mouse chest cavity after severing the aorta and the spleens were harvested. The blood was collected using 1ml pipette tips coated with Heparin and blood was loaded in EDTA tubes to prevent coagulation, and centrifuged at 4,000g for 10mins at 4°C. The blood plasma was collected and saved in -70°C. The extent of periapical lesion size and bone morphology in this model was determined on one hemi-mandible by micro CT following the protocol well described in previous study (38), after being fixed with fresh 4% PFA in PBS over night, then placed in 70% ethanol. The other half of the mandible was flash frozen in liquid nitrogen then placed in RNAlater®-ICE (Ambion, Carlsbad, CA) and transferred to -70°C for future RNA extraction and analysis.

Blood and peritoneal cells collection fro FACS

Blood was collected from WT and KO mice at 0 days as control and at different time point after exposure, 7, 14, 21 days after infection, then lysed of red blood cells using ACK buffer lysis (Thermofisher, Cambridge, MA) as follow: collected blood placed into a tube containing 10 mL of ACK lysing buffer at room

temperature for 3 – 5 minutes. After that cells centrifuged at 300xg for 5 minutes at room temperature and aspirate the supernatant, then add 5ml PBS and mix the cells for washing, finally cells centrifuged and resuspended in FACS buffer (5-10%FBS in PBS). For peritoneal cells, mice were injected with 1 ml of 4% sterile thioglycollate (Sigma-Aldrich, Natick, MA) in distilled water in the peritoneum cavity, after 24 hours peritoneum cavity lavaged with 3ml 5%FBS in PBS and collected, cells were counted and distributed in FACS tubes for analysis (see below FACS method).

Micro-computed tomography analysis (uCT)

The fixed left hemi-mandibles were scanned using compact fan-beam-type tomograph (uCT40, Scanco Medical AG, Basserdorf, Switzerland) available at the Forsyth institute. The uCT device provides a 10um nominal resolution. The imaging parameters were used as follow: Tube voltage 70 kVp, current 140 mA, and integration time 300 ms. Around 300 micro-tomographic slices were taken for each sample covering the entire structure of the hemi-mandible. Then the raw uCT data were exported to a processing computer into DICOM format, using ImageJ® program (Wayne Rasband, National Institutes of Health, Bethesda, MD), the images were angulated and re-sliced using a standard protocol to obtain a similar view between different samples. Then an image of the distal root showing the entire distal canal with a patent apical foramen chosen (showing the root and mandible bucco-lingual) and exported to Adobe Photoshop (Adobe

Systems, San Jose, CA) to measure the periapical lesion size using pre-drawn template in pixels then converted to mm^2.

Histological sample preparation and Immunohistochemistry (IHC)

Following uCT for the left fixed hemi-mandible, the same samples were washed and decalcified in 5% formic acid/10% sodium citrate. They were again washed in running water, dehydrated in a series of graded ethanols, cleared and embedded in paraffin. Six-micron serial sections of the mandibular molars were taken and every fifth section was stained with hematoxylin and eosin to identify the lesion area. Pictures of H&E were taken using Olympus BX41 microscope (Olympus, Japan).

IHC protocols were as follow:

After the desired section locations were selected (where the distal root and periapical lesion shown together) the sections were mounted on glass slides and left unstained and ready for staining. Slides were rehydrated, blocked with 0.3% H_2O_2, performed antigen retrieval as follow: put the slides in plastic box with 200ml of 0.01 M citrate pH 6.0 and heat it in a microwave under 60% power for 2 minutes, then heat for 10 minutes 10% power, after that left to cool for 20 minutes, after washing with distilled water blocked with diluted serum of the same species as the secondary antibody 1/20 in PBS, incubated with primary antibody (dilution and time varies depend on the antibody) see (Table.1), add secondary antibody as where the primary antibody species made in for 45 mins, apply ABC reagent (Vector laboratories, Burlingame, CA) for 30 mins-1 hour, apply DAB

chromogen (Vector laboratories, Burlingame, CA) for 2-10 mins or until desired staining achieved, counter stain with hematoxylin for 5 seconds or methyl green, dehydrate through serial of ethanol concentrations and xylene then mount. Washing between steps performed with PBS or distilled H_2O. Pictures were taken using Olympus BX41 microscope (Olympus, Japan).

Name	Source	Primary clone (dilution)	Incubation time	Secondary (dilution)
LY6G neutrophils	Biolegend	1A8 (1:200)	1 hour	Rabbit anti-rat (1:100) (Vector, Burlingame, CA)
CD138 plasma cells	Biolegend	(Syndecan-1) 281-2 (1:200)	Overnight 4°C	Rabbit anti-rat (1:100) (Vector, Burlingame, CA)
Smad-2P TGF-b	Biolegend	(1:200)	Overnight 4°C	Goat anti-rabbit (1.1:1500) (Vector, Burlingame, CA)
Cathepsin k Osteoclast	Borrowed (gift: John Mort)	1:500	2 hours	Goat anti-rabbit (1: 500) (Vector, Burlingame, CA)
B-220 B cell	Biolegend	RA3-6B2	2 hours	CD45R/B220 Antibody
Biotinylated IgG	Sigma	No primary		**Biotinylated** IgG

Table 1. Antibody used for immunohistochemistry.

Tartrate resistant acid phosphatase (TRAP) Staining:

Paraffin sections were deparaffinized and rehydrated through xylenes, alcohol and water. They were then Incubated in 0.2 (M) Tris buffer pH 9.0 at 37C for 1 hour, rinsing in H2O for 5 mins, followed by incubation in 0.2M acetate buffer pH 5.0 for 20 mins, then transferred to 0.2M acetate buffer containing 0.5 mg/ml naphthol AS-TR (0.025g for 50ml) and 1.1mg/ml violet LB (0.055g for 50 ml) for 30 mins-3 hours or until osteoclast are bright red, rinsed in H2O and counterstained in hematoxylin for 5 seconds, final rinsed in tap water for 5 mins, allowed to dry and mounted.

RNA extraction from bone blocks

After harvesting the right hemi-mandible from the mouse, flash frozen in liquid nitrogen, RNAlater®-ICE (Ambion, Carlsbad, CA) was added to the sample for stabilizing and preserving RNA from degradation and saved in -70°C. Under a dissecting microscope the sample was dissected of soft tissue, crown of the teeth was removed and a bone block surrounding the 1st molar and periapical lesion was made using sterile blades number 10, 11, and 15. The bone blocks were crushed using CP02 Cryoprep Pulverizer machine and tissue Tube TT1 (Covaris, Woburn, MA), the crushing repeated 2-3 times, the samples kept cold with immersing in liquid nitrogen. Then RNA were extracted using mirVana™ miRNA isolation kit (Ambion, Carlsbad, CA) following the manufacturer's protocol. 40ul elution buffer was used to concentrate RNA rather than 100ul followed by TURBO DNA-free™ Kit treatment (Ambion, Carlsbad, CA) to eliminate any DNA

contamination. RNA quality and quantity were assessed using spectrophotometers Nanodrop 2000c (Thermo Scientific, Waltham, MA) and 2100 Bioanalyzer instrument (Agilent, Santa Clara, CA).

Quantitative polymerase chain reaction (qPCR)

Complimentary DNA (cDNA) was synthesized from 650ng RNA using RT^2First strand kit (Qiagen, Hilden, Germany) and following the manufacture's protocol. We used custom RT^2 PCR profiler array (Qiagen, Hilden, Germany) with preloaded optimized primers in the 96 well plates. 13 genes and 3 controls were included in the plates. The genes list and the controls are shown in (Table.2). The controls include: GDC for mouse genomic DNA contamination, RTC for reverse transcription control and PPC for positive PCR control to make sure the machine runs the cycles as supposed. PCR components were prepared as 102ul cDNA mixed with 220ul of RT^2 SYBR green mastermix and 118ul H_2O, 25ul loaded in each well, plate were sealed, centrifuge for 1 min at 1000g room temperature, then the plate loaded in the machine and run.

Gene Symbol	Alias	Refseq #	Official Full Name	RT2 Catalog Number
Cxcl1	Fsp/Gro1/KC/ Mgsa/N51/Scyb1/ gro	NM_008176	Chemokine (C-X-C motif) ligand 1	PPM03058
Cxcl3	Dcip1/Gm1960	NM_203320	Chemokine (C-X-C motif) ligand 3	PPM34590
Cxcl2	CINC-2a/GROb/ Gro2/MIP-2/MIP-2a/ Mgsa-b/Mip2/Scyb/ Scyb2	NM_009140	Chemokine (C-X-C motif) ligand 2	PPM02969
Il1a	Il-1a	NM_010554	Interleukin 1 alpha	PPM03010
Il1b	IL-1beta/Il-1b	NM_008361	Interleukin 1 beta	PPM03109
Ly6g	Gr-1/Gr1/Ly-6G	NM_001310438	Lymphocyte antigen 6 complex, locus G	PPM68682
Il6	Il-6	NM_031168	Interleukin 6	PPM03015
Il17a	Ctla-8/Ctla8/IL-17/ IL-17A/Il17	NM_010552	Interleukin 17A	PPM03023
Tnfsf11	Ly109l/ODF/OPG/ OPGL/RANKL/ Trance	NM_011613	Tumor necrosis factor (ligand) superfamily, member 11	PPM03047
Ighg3	IgG3	NC_000078.6	Immunoglobulin heavy constant gamma 3	PPM40080
Dad1	AI323713	NM_010015	Defender against cell death 1	PPM40262
Actb	Actx/ E430023M04Rik/ beta-actin	NM_007393	Actin, beta	PPM02945
B2m	Ly-m11/beta2-m/ beta2m	NM_009735	Beta-2 microglobulin	PPM03562
MGDC	MIGX1B	SA_00106	Mouse Genomic DNA Contamination	PPM65836
RTC	RTC	SA_00104	Reverse Transcription Control	PPX63340
PPC	PPC	SA_00103	Positive PCR Control	PPX63339

Table 2. qPCR genes list and the quality controls.

The plates were run in LightCycler® 480 device (Roche, Basel, Switzerland) using recommended custom RT^2 PCR profiler array settings as follow:

Heat activation for 10 mins at 95°C and ramp rate 4.4°C/s, followed by 45 cycles of i) 95°C for 15 seconds and ramp rate 1.5°C/s and ii) 60°C for 1 min and ramp rate 1.5°C/s, then melting curve consist of i) 60°C for 15 seconds and ramp rate 4.4°C/s and ii) 95°C continuous acquisition mode (20 per °C) with ramp rate

0.03°C/s. The PCR is run for extra five cycles (i.e. 45 cycles) rather than the typical 40 cycles to allow the use of the Second Derivative Maximum method available with the LightCycler 480 software for data analysis.

Results were analyzed using ΔΔCT method as follow:

ΔCT= target gene- reference gene, then we use relative $2^{-\Delta CT}$ which gave us the relative gene expression. This performed for each target gene for each sample, then mean and standard errors were calculated. We did not take efficiency into account since the RT2 primers were optimized for high efficiency.

Fold change= $2^{-\Delta\Delta CT}$ = 2 - (average target gene (experiment group) - average reference gene (experiment group)) / (average target gene (control group) - average reference gene (control group)). = $2^{-\Delta CT \text{ exp. group}}$ / $2^{-\Delta CT \text{control group}}$.

Air pouch model

alphav KO and WT mice 8-10 weeks old male and female were used. To inflate air pouch mice were anesthetized using isoflurane, dorsal back of the mice was shaved, and 3ml of mixed sterile anaerobic gas (85% N2, 10% CO2, and 5% H2) were injected subcutaneously. The procedure was repeated twice every three days to form the pouch. After the third time of inflation $1*10^9$ CFU/mouse of mixed four bacteria species (see above, bacteria preparation) in 0.5ml PBS was inoculated in the air pouch. 24 hours later mice were euthanized and air pouch lavaged using medium containing 3ml of PBS with 10% FBS and 2mM EDTA and fluid collected for analysis. Cells were centrifuged at 400x g for 5 minutes at 4°C, supernatants were collected and saved in -70°C for later analysis, then cells

were resuspended in 2ml of RPMI 1640 with 5% FBS, counted using (Nexcelom Cellometer) via acridine orange/ propidium iodide (AO/PI) staining and cells distributed for FACS analysis. Neutrophils percentage was determined using flow cytometry FACS FITC anti-mouse Ly6G antibody (1A8, Biolegend). Bacteria were counted using drop plate method of serial dilution in PRAS (Anaerobe system) from air pouch fluid lavage before centrifuge. Taking 30ul from the air pouch fluids and putting it in tubes with 270 PRAS, then doing 10 folds dilution for 8 times (30: 270). Using Trypticase Soy Agar with 5% sheep blood plate, five drops of 10ul of diluted bacteria from all the fold dilutions were plated and left to grow for 3 days in anaerobic chamber. After that bacteria forming colony were counted from one of the five-drops dilution and multiplied by the dilution factor to get the original live CFU bacteria collected from the air pouch.

Flow cytometry FACS

After getting the desired cells from air pouch, peritoneal cavity, blood, lymph nodes or bone marrow, $1*10^6$ cells were distributed in each FACS tube, centrifuged at 400x g for 5 minutes at 4°C then resuspended in 100ul RPMI 1640 with 5%FBS or sterile 1x PBS with 5% FBS (FACS buffer). Cells were incubated with 2.5ul anti-mouse CD16/32 (antibody TruStain fcX, (BioLegend) for 10 mins for non-specific blocking, then primary antibody was added, incubated for 20-30 mins in the dark. After labeling, the cells were centrifuged, washed and resuspended in with 400ul FACS buffer, and proceeded with FACS machine

reading. Data was analyzed using FlowJo program (FlowJo, Ashland, OR). In the table below the list of antibody and the concentration used.

Antibody	Fluorophore (Clone)	Usage for $1*10^6$ in 100ul	Isotype (usage)
LY6G	FITC (1A8)	2.5ul	IgG2b
LY6G/LY6C	PE (RB6-8C5)	1ul	IgG2b
F4/80	Alexa488 (BM8)	2ul	IgG2a
CD11b	APC (M1/70)	Mix1: 1 then use 1ul	IgG2b
alphav	PE (HMa5-1)	1ul	Armenian Hamster
alphav	PE (RMV7)	1ul	IgG1
Cxcr2	PE*	2.5ul	IgG2a
CD19	Alexa488 (6D5)	Mix1: 1 then use 1ul	IgG2a
CD3	FITC (17A2)	2ul	IgG2b
CD 138	Syndecan-1 APC (281-2)	2ul	IgG2a

Table 3. Antibody used for FACS.

Note: regarding (HMa5-1) PE antibody from Biolegend, it has been shown it recognize alphav not alpha5 (76)

The enzyme-linked immunosorbent assay (ELISA)

For total IgG and IgG3 eBioscience kits Mouse IgG total Ready-SET-Go! ® were used (eBioscience, Vienna, Austria) and the manufacturer's protocols were followed. The plate was read using ELISA POLARstar Omega Plate Reader and data analyzed using Graph-Pad Prism (Graph Pad Software, La Jolla, CA).

For bacteria specific antibodies: a protocol prescribed in previous paper was used (39) as follow: bacteria species were grown in anaerobic chamber for 3-4 days, resuspended at an OD 600 of 0.3 in sterile PBS, and fixed in 3 ml of 4% PFA. After washing three times with 3ml 1x PBS, 100ul of bacteria were added to the wells of a 96 high binding plate (manufacturer, catalog #) for 3 hours in 37°C, and then incubated for two days in 4°C. The plate was then washed three times with (0.9% NaCl, 0.05% Tween 20), blocked with 1% BSA in PBS with 0.05% Tween (PBST) for 2 hours, and washed with PBST three times. Diluted serum from KO and WT in PBST (1/400, 800, 1600, 3200) was added to each well and incubated for 2 hours at room temperature with shaking. After three washes with PBST, 100ul diluted goat anti-mouse IgG conjugate (Bio-Rad, Hercules, CA) (1/3000 dilution in PBST) was added and incubated for 2 hours. After a final wash 7 times with PBST, 100ul TMB substrate reagent set (BD Sciences, San Diego, CA) was added and color was allowed to develop for up to 20 mins, 50ul 1M phosphoric acid was added, and OD at 450 nm was measured using ELISA POLARstar Omega Plate Reader Spectrophotometer (BMG Labtech, Germany).

Fluorochrome Bone labeling

To view new bone formation at different time point in vivo mice were injected IP with 0.1ml (90mg/kg) Xylenol orange at day 13-14 and 0.1ml (5mg/kg) Calcein at day 18 after infection. Mice were euthanized at day 21-22, and jaws were collected, and fixed in 70% ethanol at 4°C overnight. They were then transferred to 95% ethanol for 30 mins for 2 changes, 100% ethanol for 30 mins for 2 changes, acetone for 30 mins for 2 changes, then embedded in with Technovit 8100 or Technovit 2000 LC (Heraeus Kulzer, Germany) following the manufacturer's recommendation. Briefly an infiltration liquid was mixed, placed with the sample in a tube, agitated for 2 hours with 2 changes at 4°C, third change under vacuum pressure over night, mixed hardening solution and placed the sample in plastic molds, sealed with parafilm or tin foil, allow it to set over night at 4°C. The blocks were then sawed into small sections and attached to histology glass slides and viewed with a wide-field microscope Axio Observer Z1 (Zeiss, Germany).

Statistical analysis

Mean and standard error were calculated for statistics description. Unpaired t-test was used for two-group comparison, and one-way ANOVA for multiple group comparison followed by post-hoc Tukey's test to identify differences between groups. Data were analyzed using Graph-Pad Prism 4.0 (Graph Pad Software, La Jolla, CA).

Results

alphav knockout confirmation

Breeding for experimental mice was not giving adequate number of pups compared with breeding for $av^{flox/flox}$ (WT) or homozygous av-tie2cre. Mating cages for experimental mice gave birth to an average of 15.22 pups (including experimental and littermates control) based on 9 mattings while for $av^{flox/flox}$ was 24.25 pups based on 4 mattings in around 6 months period. The veterinarian were not able to locate the issue and the necropsy report was negative for know conditions or viruses.

In order to verify the conditional knockout in the mice, genotype was analyzed using PCR for ear tissue and showed $av^{+/-}$, $av^{flox/+}$, and Tie2Cre+ for knockout experimental mice, while littermates showed av+/+, $av^{flox/+}$, and Tie2Cre+ which used as control. Cells were collected from three different sources: bone marrow neutrophils, peripheral blood cells and the inflamed peritoneum. Flow cytometry was used to determine alphav expression on neutrophils by gating for Ly6G expression. The results showed a lack of alphav expression in the knockout neturophils in all three compartments, compared to strong expression in the control littermates neutrophils (Figure 2, 3), confirming complete knockout of alphav integrin in neutrophil cells in KO mice and normal alphav expression in WT mice.

Development of periapical abscess. Pulp exposure of mandibular 1^{st} molar and inoculation of the four bacteria species (*Prevotella intermedia, Fusobacterium nucleatum, Streptococcus intermedius,* and *Parvimonas micra*)

was performed in WT and KO mice to investigate the role of alphav on immune cells in periapical lesions development and response. Mice were sacrificed at 0, 7, 14, and 21 days after infection. Strikingly, αv-tie2cre (KO) experimental mice developed abscess and swelling at the site of infection in 6 out of 16 mice in 21 days group, while in wild type none of the mice developed abscess out of 18 mice. (Figure 4) shows the dissected head of an αv-tie2cre mouse showing abscess with pus accumulation in periapical area of 1st molar (mice sacrificed at 21 days post infection). Abscesses developed between day 14 and day 21, and from the first experiment group performed out of 3 KO mice one was already dead by day 21. After that experiment mice were monitored on daily basis after day by daily weighing and assessment of body condition. Mice that developed abscesses lost weight and were looking weak, and were sacrificed when these symptoms were identified. These results indicate that knockout mice that lack alphav in immune cells were unable to contain and include the infection to the periapical area and developed abscess and systemic phenotype.

Ectopic bone formation. After sacrificing mice, uCT was used to determine the bone structure in the infected mandibles. The KO mice exhibited irregular bone formation (we are going to call it ectopic bone) on the lower border of the mandible, most likely as a reaction to the endodontic bacteria infection. The ectopic bone formation started to show in some KO mice sample at 14 days after infection but became clear in 21 days samples compared to WT, which showed little or no ectopic bone formation. Figure 5 shows representative 21 days uCT samples for both groups. In the KO group clear bone formation is observed

below the inferior border of the mandible with trabeculation and weak density, suggesting that this bone resembles cancellous bone rather than compact bone. The cases of mice showed the ectopic bone formation in 21 days is presented in (Figure 7).

Periapical lesion size was defined as amount of bone resorption around distal root apex measured from uCT. The measurement and analysis of periapical lesions size in WT and KO from uCT shows similar lesions size between KO and WT and there is no significant difference in any time point of the experiment between the two groups (Figure 6). Although the periapical lesion size was not different between the two groups, KO mice developed unusual ectopic bone formation in 21 days as result of intense inflammatory reaction to the infection.

Mice were injected with bone labeling fluorochromes to demonstrate that the ectopic bone observed resulted from new bone formation. Fluorochromes xylenol orange and calcein were incorporated into new bone formed between days 13-18 and days 18-22, as we injected xylene orange at day 13 and calcein at day 18 and mice were sacrificed at day 22. We used wide-field fluorescence microscopy to show the bone formed between the two periods labeled with different color. The results (Figure 8) at 100x magnification represent are the lower border of the mandible of αv-tie2cre (KO mice) sacrificed 22 days after infection. Orange color line can guide as a base line from day 13-18 and then green color represent the bone formed between days 18 and 22. Using labeling fluorochrome is consistent with the ectopic new bone formation resulted as a reaction to endodontic infection in KO mice occurred between 13 and 22

days after pulp exposure. However, comparison with infected WT mandible is required to confirm this result.

H&E staining were made to give a generalized histological characteristic about infected mandibles. General histological view showed inflammation involving a wider area of the mandible, and deformation to the mandible bone morphology in KO mice (Figure 9). Also, these images show a loss of smooth lower border of the mandible and replacement of thick compact bone by a spongy newly ectopic bone in KO, rather than just inflammation and bone resorption around the periapical area as seen in WT as target for analysis in endodontic infection of the mouse model. H&E staining showed wider area of reaction to the induced infection in KO mice more than periapical bone resorption.

Neutrophils staining was performed to investigate the effect of alphav on neutrophils migration to periapical lesions. Ly6g IHC staining for neutrophils showed a significant reduction in neutrophil cells number presented in periapical area 21 days after infection in KO mice compared to WT littermates measured from three fields area around distal root apex (Figure 10).

Neutrophils tendency to have reduce migration in air pouch model. We further tried to explore the cause for the intense inflammatory response seen in the alphav KO mice. Since it is difficult to extract cellular infiltrate or collect bacteria from the small periapical lesion we used the well established air pouch model to investigate neutrophil migration to sites of endodontic infection. Experiments were performed on 8 WT and 6 KO 8-10 weeks old mixed male and

female mice. Air pouch was made on the dorsal back of mice by inflating 3ml of anaerobic mixed gas few times, then $1*10^9$ CFU/mouse of mixed four bacteria species (*Prevotella intermedia, Fusobacterium nucleatum, Streptococcus intermedius,* and *Parvimonas micra*) was injected. 24 hours later air pouch lavaged and fluids were collected. Cells recovered from air pouch were counted and showed around 35% less cells collected in KO mice compared to WT but the difference was not statistically significant due to large variability in cell numbers recovered from individual mice (Figure 11a). Around 75-80% of the migrated cells to the air pouch are neutrophils analyzed using flow cytometry FACS with FITC Ly6g antibody (Figure 11b). Fluids collected from the air pouch were tested for live bacteria using drop plate method and showed no difference in bacterial enumeration (Figure 11d). Despite there is no statistical difference in the neutrophils number collected from air pouch between KO and WT, there is clear trend toward reduction in neutrophils number recovered from air pouch.

TRAP staining was obtained to count for osteoclast numbers in periapical lesions and determine if alphav has effect on their formation. TRAP did not show a difference in osteoclast numbers between the αv-tie2cre experimental and WT control groups in 21 days samples around periapical area (Figure 12). Osteoclast function could be affected from lack of alphav and Pit formation assay or similar test will be performed to test for osteoclast function. Osteoclast formation seems normal around periapical lesion determined through counting osteoclast number.

Cytokines and chemokines expression. After observing severe phenotype in KO mice, we performed qPCR to investigate for known inflammatory cytokines and chemokines changes in the periapical periodontitis. We tried to explore the expression difference between KO and WT mice in inflammatory mediators related to neutrophils, macrophages and bone resorption activity. RNA was extracted from periapical area bone blocks from all time point, and then cDNA was made and analyzed by qPCR using optimized primers. Data from day 14 (no. WT=5, KO=7) revealed significantly increased expression of cxcl1, cxcl2, IL-1a, IL-6 and RANKL genes in KO compared to WT; results were normalized to Dad1 (defender against cell death 1) as a reference gene (Figure 13a). These mediators are pro-inflammatory and lead to increase immune response to the endodontic infection causing more damage and bony destruction. IL-1a and IL-6 has the highest fold increase in 14 days with 3.9 and 4.9 folds increase (Figure 13c), respectively. From day 21 data (n. WT=6, KO=7), there was no significant difference in genes expression between KO and WT mice in the tested cytokines and chemokines. In (Figure 13) all data for the different immune mediators is presented for 14 and 21 time points. Gene expression and fold changes analyses were performed between the experimental KO group and WT control samples collected at the same time point. Strict quality control criteria were applied, as many samples did not pass the RTC (reverse transcription control) and few did not pass GDC (genomic DNA contamination) and were taken out of calculation in 14 and 21 days groups. In 0 and 7 days most samples did not pass the quality control criteria.

Indication of defect in B cells migration or function. Since there was no studies report av-tie2cre KO role in dental and oral diseases we requested to do microarray to look into overall phenotype for this KO regarding periapical lesion. 3 WT and 3KO RNA samples extracted from bone block surrounding the periapical area of 1st molar tooth 21 days after infection were sent for microarray unit for analysis. Using Mouse Gene 2.0 ST arrays, 1 WT sample did not pass quality and normalization assessments and was excluded. Around 25,000 genes were tested and many pathways were analyzed. The expression of Itgav (alphav) was 2.1-fold lower in the three knockout samples than in the two remaining wild type samples (a 53% decrease in expression), the expression not completely absent due to presence of non-hematopoietic cells like fibroblast in the periapical area. In (Table. 4) show results for overexpressed gene that has fold increase more than 5 and p-value<0.05, there were only a few genes in this category; such as cxcl3 which was over expressed 13 fold in KO compared to WT. Also, two Keratin genes showed up regulation and they could be from gingival tissue left behind in the bone block. On the other side for under expressed genes we predicted an immune system defect due to deletion of alphav in immune cells. We observed an interesting robust down expression of genes related to B cells going to up 55 fold decrease in KO compared to WT. In (Table. 5) is presented a list of the genes that has more than 5 fold decrease and p-value<0.5, all these genes are related to B cells except one is T cell receptor related.

As we detected strong down regulation for many B cell related genes we analyzed blood plasma for IgG level. Using blood plasma collected when

sacrificing the mice we tested the level of IgG3 as it was the most down regulated in the microarray data, as well as total IgG using ELISA. The data showed a big variation amongst individual animals although it was repeated four times (Figure 14); it is unclear if the variation could be an issue with the kit itself. Despite the difficulty to draw a conclusion, there was a tendency for reducing in both antibodies production total IgG, and IgG3 in the blood plasma in KO mice compared to WT in 14 and 21 days post infection.

Mandibular Lymph Nodes shows decrease in B cell percentage. As blood plasma IgG's could be a systemic impact, we wanted to look for more local effect related to the endodontic infection. After 21 days of inducing endodontic infection, mandibular lymph nodes were isolated and single cell suspension obtained. The cells were analyzed for CD19 (B cell) and CD3 (T cell) using flow cytometry FACS (2 mice per group), the result showed a slight reduction in B cells percentage (Figure. 15a), while no change in T cells (Figure 15b). Also, we investigate the number of plasma cells in air pouch model collected fluids, in experiment of 5 mice (3 WT, 2KO) showed a reduction in plasma cells percentage and number collected from the air pouch fluids using FACS analysis with CD138 antibody (Figure 16a, b).

Specific bacteria IgG. We wanted to look for blood plasma level for specific bacteria antibody in WT and KO in vitro to find if KO had lower antibody activity to WT. We coated high binding plate with the four bacteria species *Prevotella intermedia, Fusobacterium nucleatum, Streptococcus intermedius*, and *Parvimonas micra*, which we used for inoculation during pulp exposure

procedure, each one separately. First we tested diluted blood plasma (1/100, 1/200, 1/400, 1/800) from WT and KO control samples, without pulp exposure or inoculation of four bacteria species, to see if the mice have antibody to the specific bacteria before infection. (Figure 17a,b) showed mice already have antibody activity with *Streptococcus intermedius*, and *Parvimonas micra* as the antibody level were similar in 21 days WT blood plasma after infection, while with *Prevotella intermedia*, and *Fusobacterium nucleatum* there were increased in antibody reactivity in 21 days WT blood plasma after infection (Figure 17c,d). This results indicating the mice developed more antibody for *Prevotella intermedia*, and *Fusobacterium nucleatum* after pulp exposure and infection. The increased in activity with *P. intermedia* is the highest also, the different response of 0 day WT and KO to *Fusobacterium nucleatum* at baseline is interesting, but maybe this is just mouse-mouse variation. Then, we tested antibody activity of diluted blood plasma (1/400) from 21 days WT and KO to *Prevotella intermedia.* The results showed lower antibody activity in KO compared to WT, but the results need to repeat with lower dilutions (Figure 18). This results support the previous results indicating defect in B cells in KO compared to WT.

Discussion

alphav is a receptor for multiple ligands and it affects numerous cellular processes such as differentiation, migration, adhesion and survival (51, 52). alphav importance in controlling inflammatory process in immune cells has been shown, as mice with myeloid cells lacking alphav develop colitis resulting from a lack of activated Treg to control and balance the gastrointestinal tract system immune homeostasis and phagocytosis dysfunction of macrophages and dendritic cells (56). Conditional alphav knockout mice have been developed as complete KO mice die at or shortly after birth. In our experimental mice we used Tie2, a promoter for hematopoietic cells to study the effect of alphav in immune cells.

Endodontic infection or periapical periodontitis is good model to study as it resemble different body infection, and majority of cellular infiltrate in the periapical area are immune cells and the other are healing repair cells (18, 19).

Our results show the importance of alphav integrin in endodontic polymicrobial infection and its role in controlling infection from being disseminated. 6 out of 16 mice developed abscess and swelling in the 21 days group after infection, these mice lost weight and exhibited malaise, which lead us to sacrifice some of them before they complete their assigned time point. Although periapical periodontitis model has been studied widely, to our knowledge there are very few knockout mouse model that developed a similar

severe phenotype. Severe combined immunodeficient SCID (RAG-2) with immature B and T cell functions were reported to develop abscesses (38). Interestingly, B cell deficient (Igh-6) mice also developed orofacial swelling and suffered weight lost which lead to death of some of the mice indicating disseminating infection and blood septicemia (39). These results are consistent with our data suggesting a defect in B cell function in the absence of the alphav integrin.

In a study to investigate the role of OPN in endodontic infection OPN knockout mice developed a larger lesion size compared to WT, as the immune system was deteriorated as results of neutrophils defect in the periapical area (46). Also it has been reported that OPN deficiency led to macrophage killing dysfunction and reduced their ability for bacteria and damaged tissue clearance (77, 78). Po-inflammatory cytokines and bone resorption modulators IL-1a and RNAKL expression in periapical area were up regulated in that model. The role of OPN on myeloid cell phagocyte ability should be mediated by its ability to bind to integrins av, a9, and a4 in these cells (79-81). Also, it has been shown that OPN is a high affinity ligand for alphav integrin (50), from that we wanted to investigate the role alphav in periapical periodontitis induced in a mouse model and we expected that it has similar protective role in this model which has not been shown before and gain more knowledge about the integrin role in endodontic infection.

Here in our study, neutrophils number in periapical area was reduced in KO mice as detected by IHC compared to WT, which indicate a defect in the migration or

chemotaxis process for PMN. A similar result has been shown in P-, and E-selectin KO mice with increased periapical inflammation and expression of a main pro-inflammatory cytokine IL-1a, which also shown in our study (29). Although our data from air pouch model to test neutrophils migration failed to show a significant difference (due to variation in cells number collected from mouse-mouse and small samples no (6 KO and 8 WT)) but there was a trend for neutrophils number reduction in KO which is similar to results seen in OPN KO study, where mice lacking OPN showed reduction in neutrophils number collected from peritoneal cavity compared to WT (48). Reduced neutrophils infiltration in the periapical area could be result from a lack of OPN function on the cells mediated by the alphav integrin.

Gene expression analysis showed increased proinflammatory cytokines IL-1a, IL-6, cxcl1, cxcl2, and RANKL in 14 days KO mice compared to WT indicating up regulation in inflammatory response in KO. IL-1a and RANKL has been shown to be upregulated in different models where there are associated with increase inflammation and more bone resorption area in periapical periodontitis. Thus, these results are consistent with results indicating IL-1a and RANKL up regulate inflammation and bone resorption reported in different models.

The microarray data showed a down regulation and potentially a defect in B cells ability to produce antibody which may explain why these mice are unable to control the infection as they develop swelling and developed systemic symptoms, rather than just local periapical bone resorption and inflammation as seen in most of this model studies results. The B defect and inability to produce

antibody was the cause for disseminating infection and systemic effect in a mice study performed by Stashenko group in (Igh-6) KO mice (39). The mice phenotype was largely recovered by transferring enriched antibody to the mice before the infection induced in their study.

Blood plasma total IgG and IgG3 showed indication for reduction in day 14 and day 21 samples collected at the time of sacrificing (not statistically significant), also our data suggest that percentage of B cell is lower in the KO mice compared to the WT in mandibular lymph nodes which is more local and related to oral infection drains. Also, our preliminary data showed 1/400 diluted blood plasma collected from 21 days KO mice had lower antibody activity to*, Prevotella intermedia* compared to WT which could enforce our results suggesting defect in B cell function. The experiment needs repeat with lower dilutions and to confirm the results. Although plasma cells level in the air pouch is low, it seems a decrease in av-tie2cre mice to WT. Many of the B cell experiments are not conclusive, and need to be repeated with more samples including B cell analysis from lymph nodes, ELISA of blood plasma for IgG's, ELISA of bacteria specific antibody activity in blood plasma. Nevertheless, when taken together they all indicate a decrease in B cell accumulation or function.

It has been shown that alphav on dendritic cells is required for TGF-b activation through its avb8 integrin, which necessary for repair of damaged tissue and regulation of the adaptive immune response (60) through its role in local activation of Treg cells. These results were generated using the same mouse (av-tie2cre), where colitis development at later times was observed. Treg has

been reported to up regulated in periapical periodontitis but its role has not been reported (82). The effect of alphav KO in immune cells on Treg presence and regulation in periapical area should be evaluated in future study.

Also, DC alphav activation of TGF-b is required for Th-17 activation, a main source for IL-17 production, which has been show to recruit neutrophils through different chemokines like cxcl1, cxcl2 (42, 83). In a mice study where IL-17 RA was deleted, there was increased bone resorption in periapical area, and IL-17RA was determined to play a protective role in endodontic infection (41). In our study there were no change in IL-17a in periapical tissue using qPCR gene expression, but there were increases in expression of IL-1a, and cxcl2 similar to the result seen in IL-17RA KO study. A defect in DC function in av-tie2cre could be responsible for the B cell phenotype, as DC involved in B cell initiation and regulation of antibody production directly or through T cell dependent activation (84)

Formation of periapical lesion happens as immune defense mechanism to contain the infection after dental pulp fails to repress the invading bacteria. Although, existence of the lesion around root apices is considered indication for presence of infection and immune activity in human clinical evaluation, lesion size are not always indication for severity of infection or immune response as seen in human clinical cases where patients develop abscesses without presence of large lesion size. Our results here support that idea where av-tie2cre mice has similar periapical lesion size compared with WT despite that av-tie2cre developed intense reaction including swelling and abscess and ectopic bone

formation in 21 days. Defect in osteoclast function could explain why the av-tie2cre mice did not develop larger resorption area around infected roots to contain the infection. Also, the mice developed unusual ectopic bone formation around lower border of the mandible in response to the infection in av-tie2cre mice, this could be due to defect in osteoclast function and imbalance in bone remodeling process as a result of failure of immune system to fight infection. TRAP staining result showed osteoclast differentiation and presence around periapical area was similar between KO and WT mice and was not affected by alphav knockout from immune cells. In future study osteoclast function from av-tie2cre will evaluated.

Conclusion

- av-Tie2cre KO mice developed abscess and swelling formation (disseminating infection) reaction to pathologically induced periapical periodontitis.
- av-Tie2cre KO mice showed reactive ectopic bone formation, likely due to intense inflammatory response to endodontic infection.
- Defect in neutrophils migration in av-tie2cre supported by reduced number of neutrophils in periapical lesion and air pouch results.
- Defect in B cells in functions or migration might have caused the abscess formation supported by result from microarray, reduced percentage of B cells in lymph nodes, from blood plasma IgG's and specific bacteria antibody activity results.
- alphav integrin on hematopoietic cells plays protective role and involved in modulating immune response in endodontic infection.

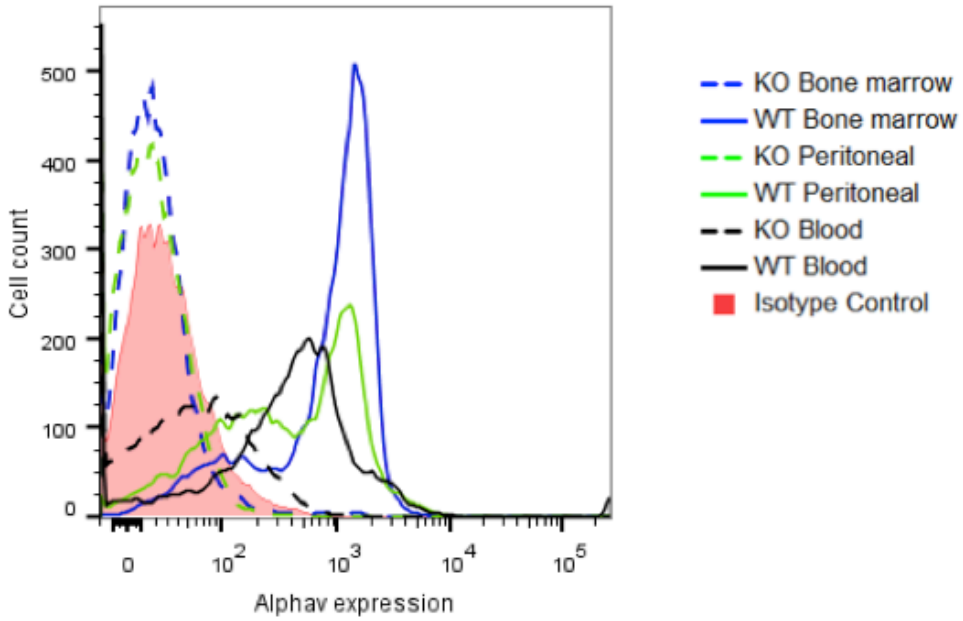

Figure 2. Lack of alphav expression in neutrophils confirmed using FACS with CD49e (HMa5-1) in cell gated on LY6G (1A8) in αv-tie2cre KO mice compared to WT mice in blood, bone marrow cells and peritoneal cells

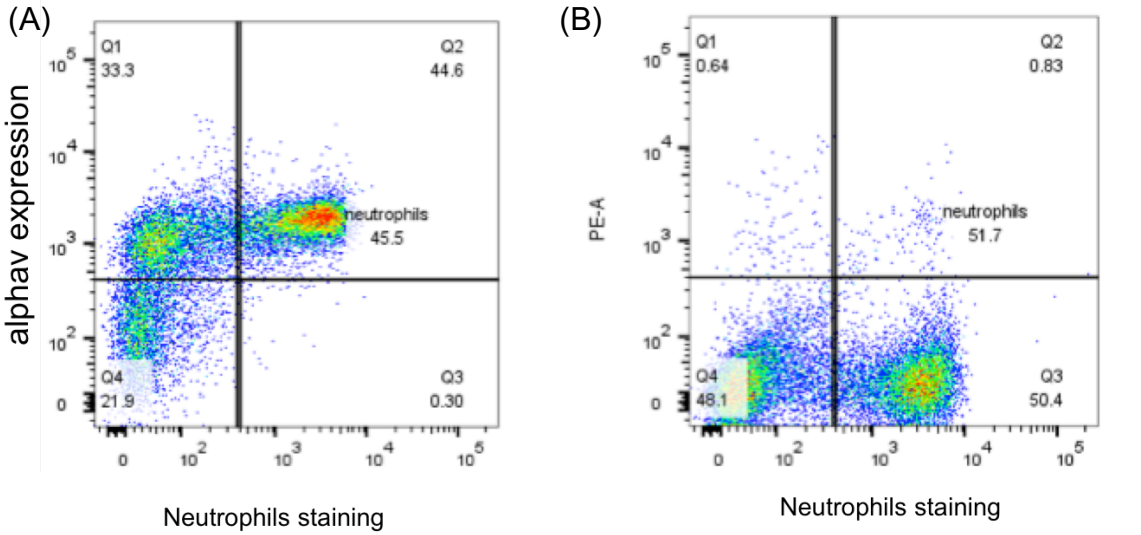

Figure 3A and B. Histogram showing lack of alphav expression in neutrophils confirmed using CD49e (HMa5-1) and gated LY6G (1A8) staining FACS in αv-tie2cre KO mice (b) compared to WT mice (a) in bone marrow cells.

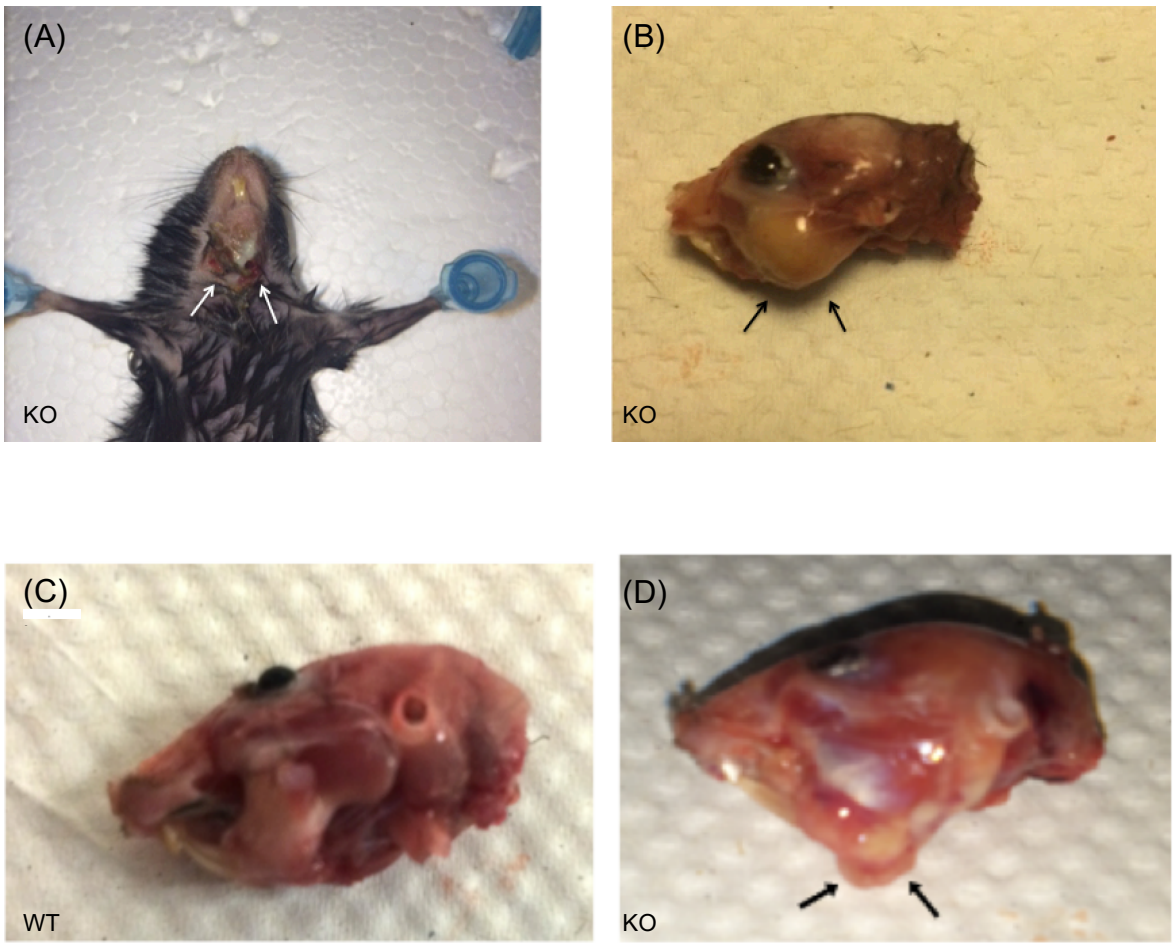

Figure 4. Images of αv-tie2cre mice showing abscess with pus formation in periapical area of 1st molar in (a, b, d) (sacrificed at 21 days) compared to WT (c). Arrows pointing to the abscess area where there is pus accumulation.

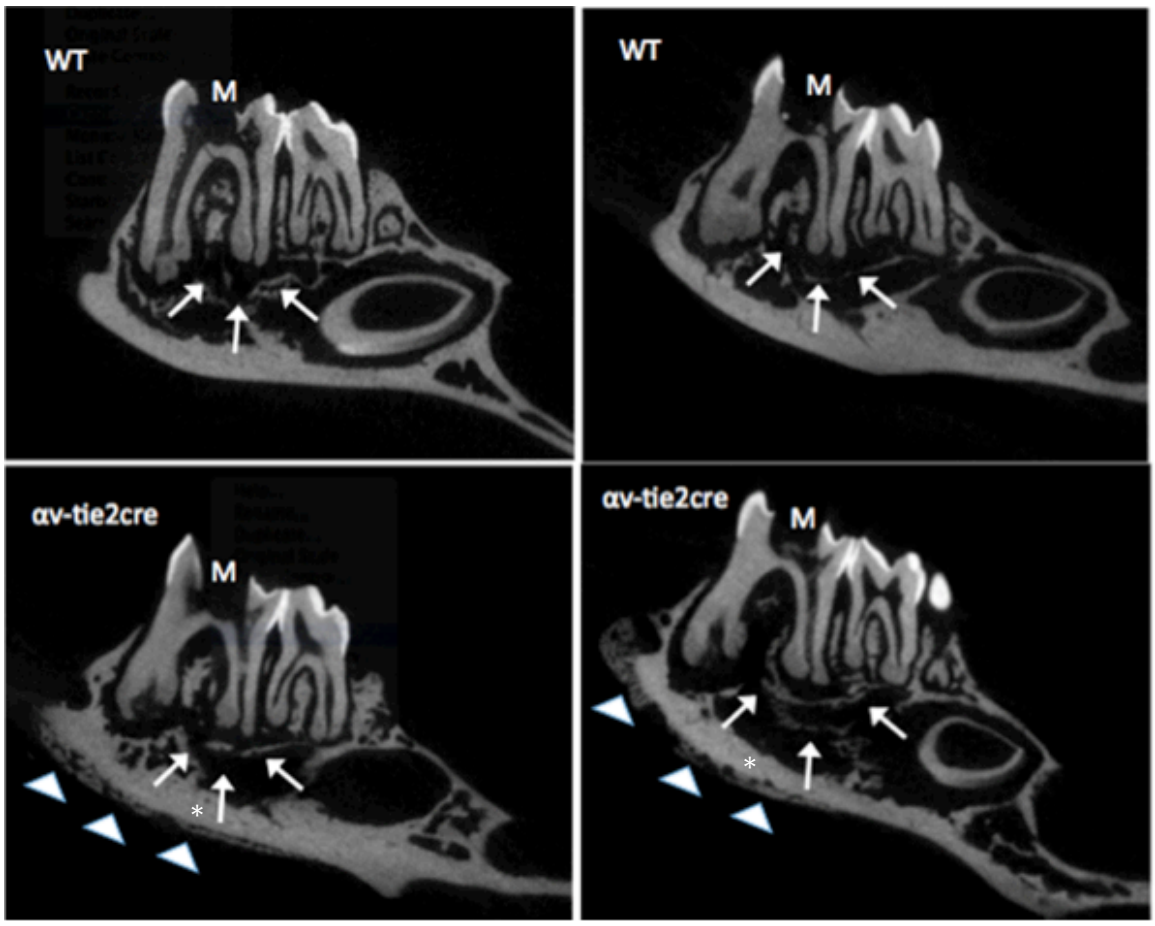

Figure 5. αv-tie2 mice have bone destruction after pulp exposure, accompanied with ectopic bone formation on the lower border of the mandible. Micro CT images of mandibles from exposed and infected WT (top) and αv-tie2 mice (bottom). M indicates first molar. Arrows indicate area of bone loss around distal root periapical area. Arrowheads indicate ectopic bone formation. Asterisks indicate bone loss in the lower part of the mandible.

(A)

(B)

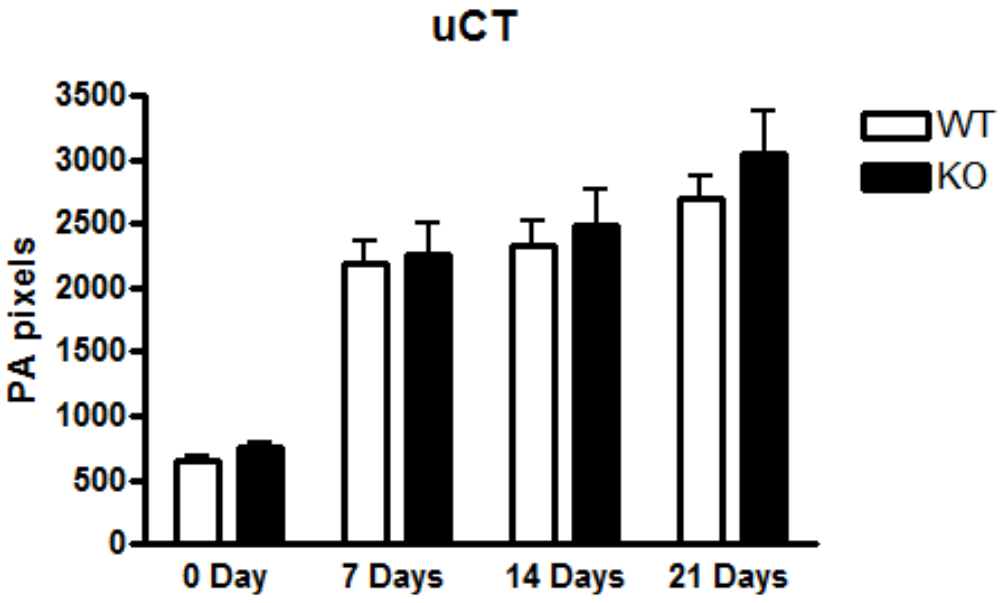

Figure 6. Periapical lesion size was measured from uCT images using ImageJ and Photoshop programs, (a) example how periapical lesion size was measured. (b) Mean for periapical lesion size in different time points, there was no difference in lesion size between the KO and WT in any experimental time points.

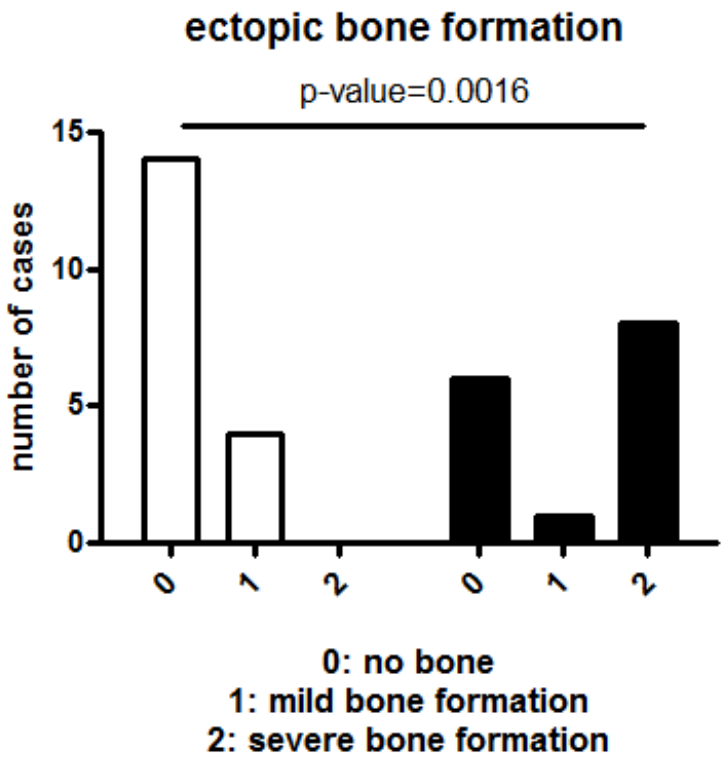

Figure 7. Ectopic bone formation cases, number of mice exhibited irregular ectopic bone formation on the lower border of the mandible in 21 days post infection in KO and WT mice. ectopic bone formation grade estimated from uCT images. (p-value= 0.0016).

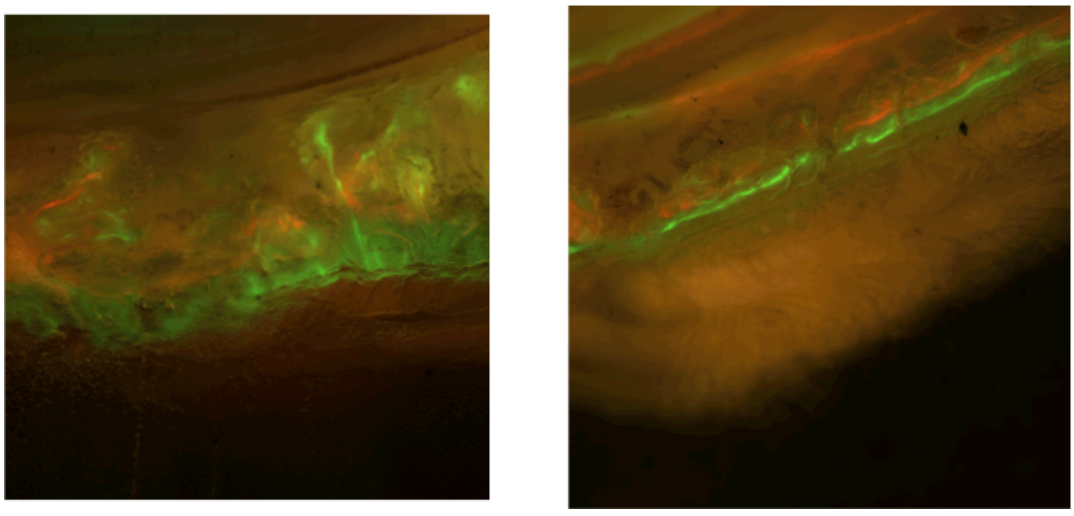

Figure 8. Wide-field pictures showing ectopic bone formation in KO mouse using two labeling fluorochromes, xylenol orange (orange) injected at day 13 and calcein (green) injected at day 18 after infection, mice sacrificed at day 22 (100x). Left image show irregular bone formation consistent with uCT images and the right shows more linear bone formation.

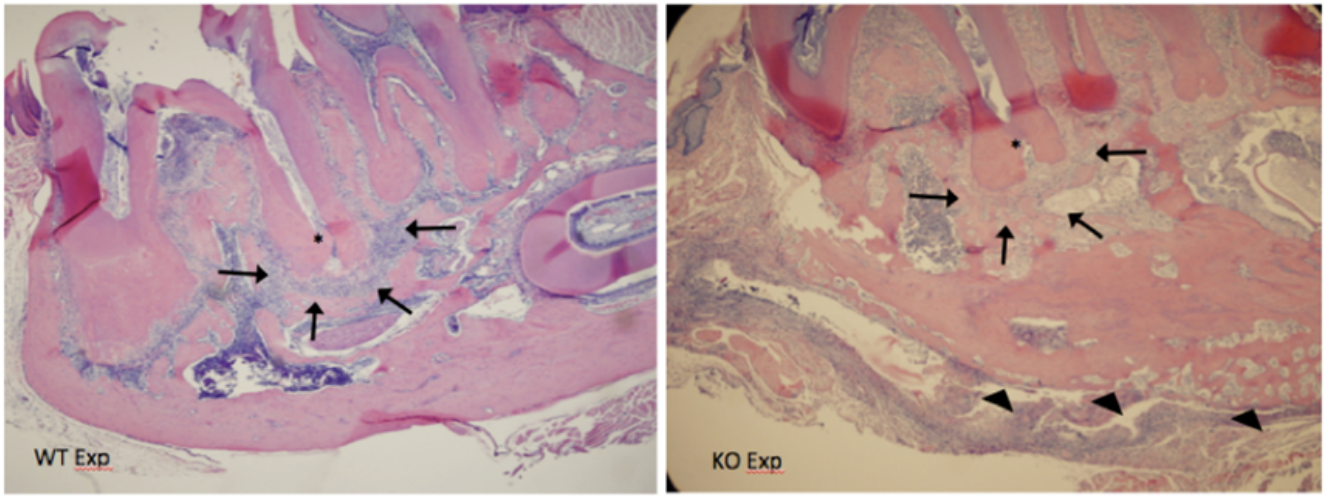

Figure 9. αv-tie2 mice have inflammation after experimental infection beyond periapical area compare to WT where it is limited to periapical area. H+E staining of mandibles from exposed and infected mice 21 days after exposure. An asterisk indicates the first molar distal root apex. Arrows indicate the area of inflammation. Arrowheads indicate ectopic bone formation. (40x)

(A)

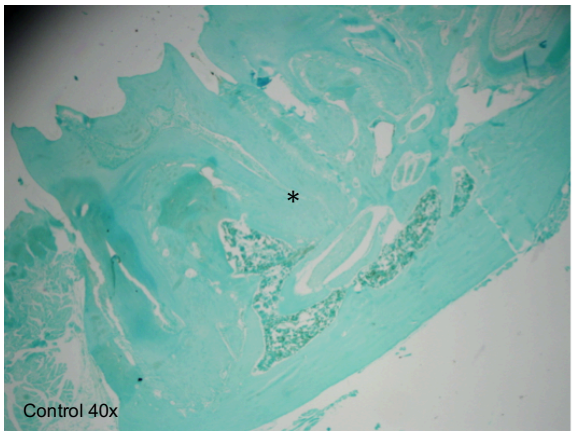
Control 40x

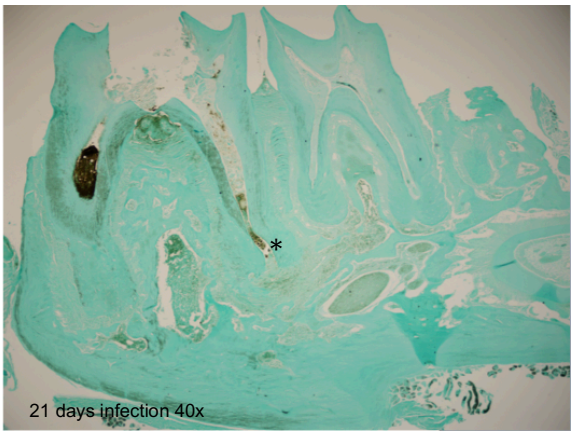
21 days infection 40x

(B)

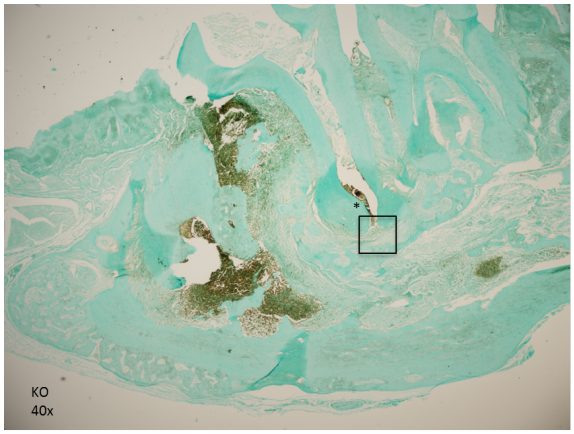
KO
40x

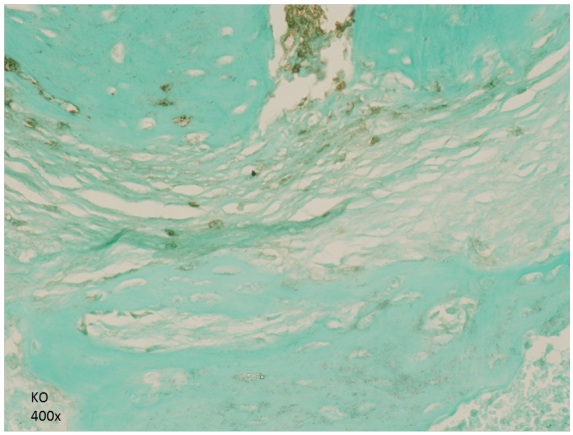
KO
400x

(C)

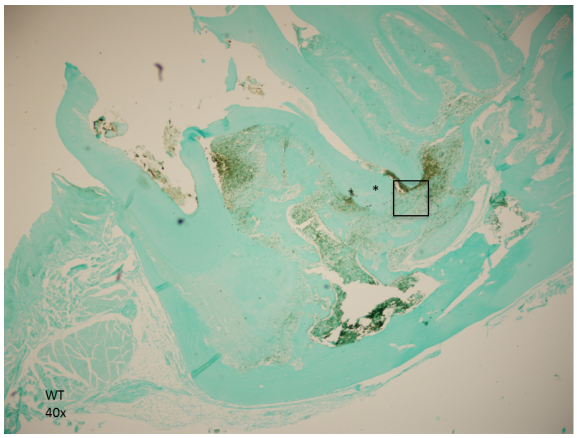
WT
40x

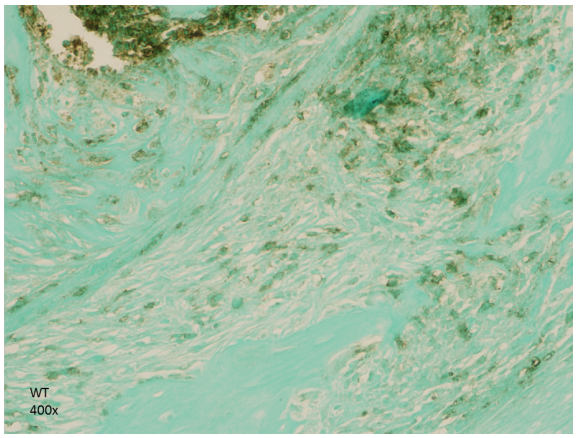
WT
400x

(D)

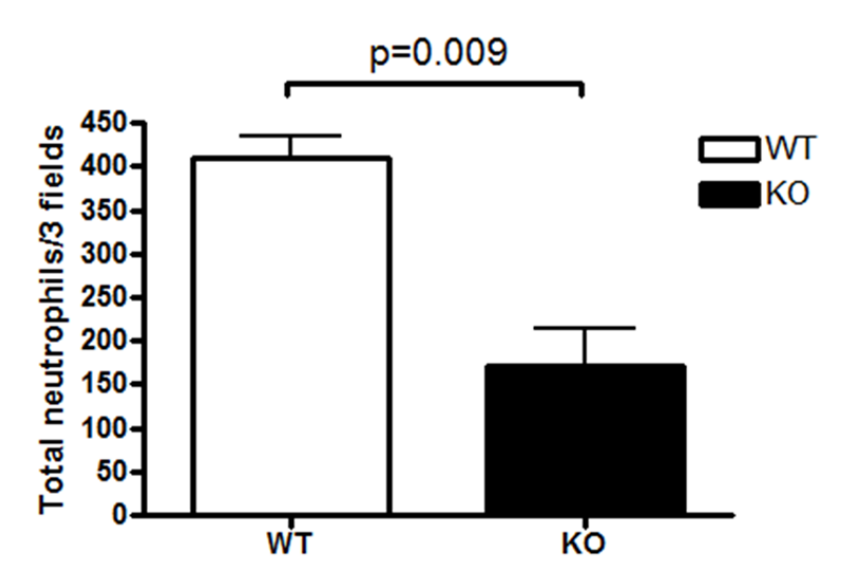

Figure 10. IHC staining using Ly6g antibody. (a) Image of 0 day with no pulp exposure showing normal periapical area and no neutrophils infiltration or bone destruction, and 21days after infection showing neutrophils infiltration. (b) Images of 21 days KO after infection 40x and 400x for one field around distal root area. (c) Images of 21 days WT after infection 40x and 400x for one field around distal root area. (d) Reduction in neutrophils cells number presented in periapical area 21 days after infection in KO mice compared to WT measured from three field area around distal root apex using 400x pictures. An asterisk indicates the first molar distal root apex (p-value=0.009).

(A)

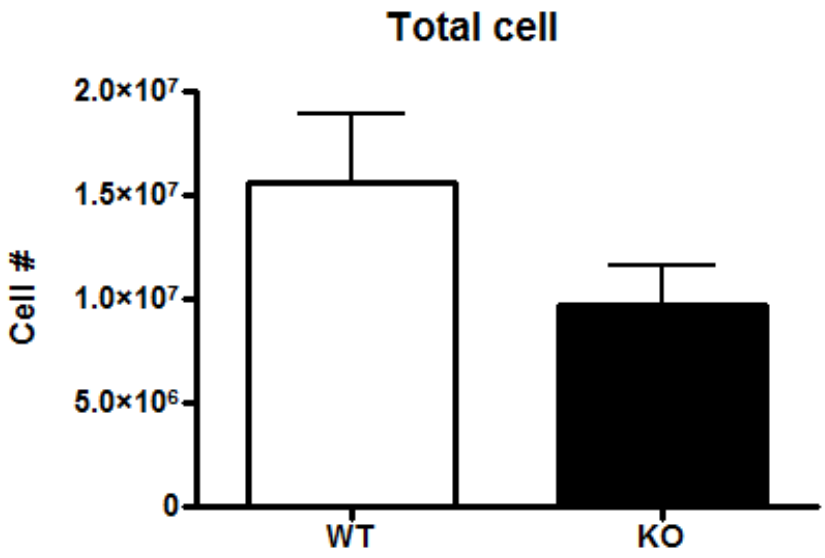
Total cell
2.0×10⁷
1.5×10⁷
1.0×10⁷
5.0×10⁶
0
Cell #
WT
KO

(B)

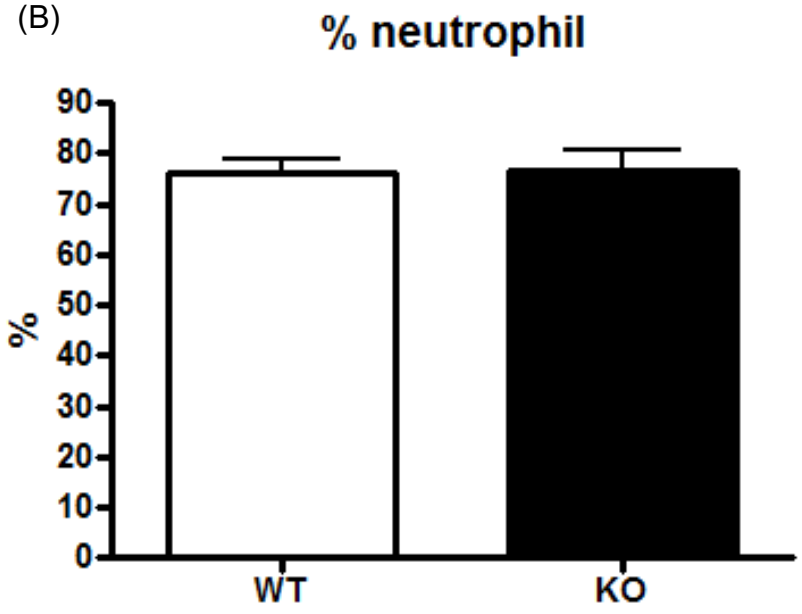
% neutrophil
90
80
70
60
50
40
30
20
10
0
%
WT
KO

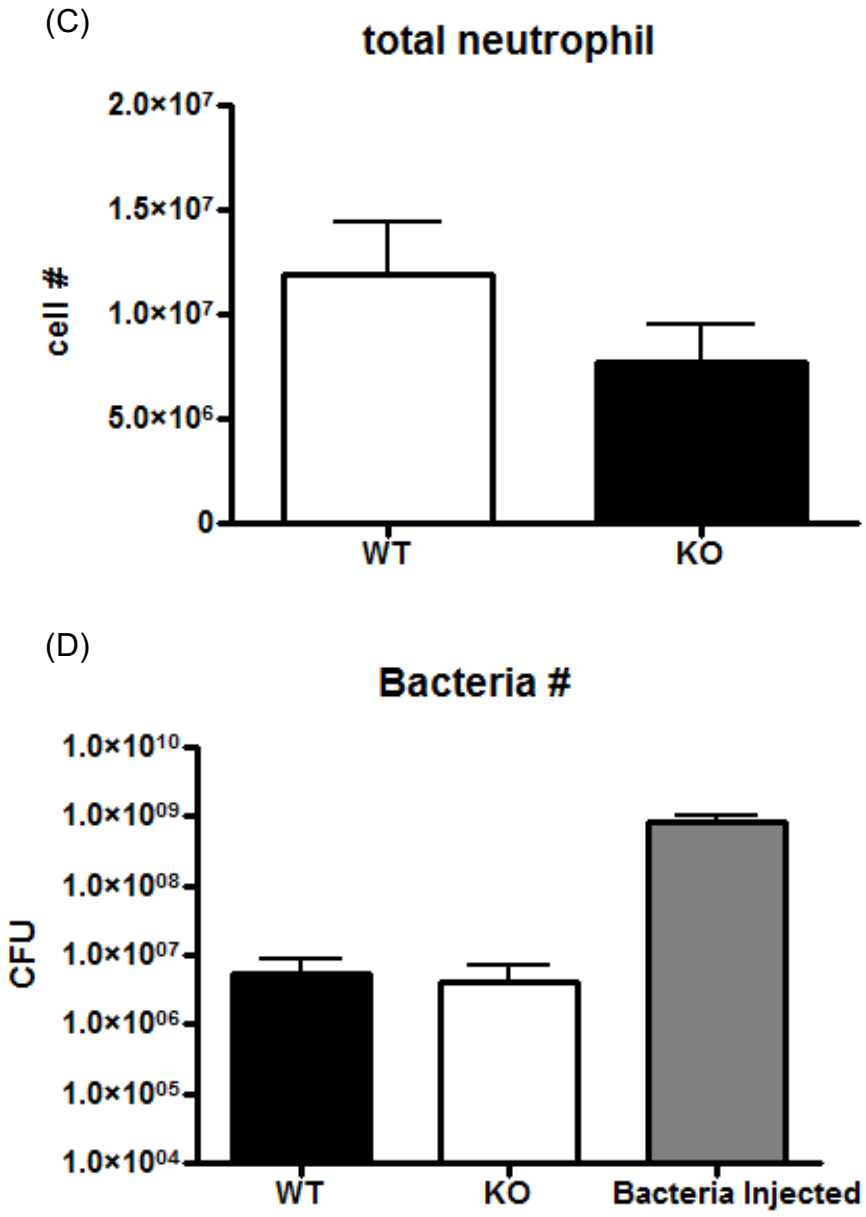

Figure 11. (a-d). Air pouch experiment data. (a). Total cells number collected from air pouch, counted using (Nexcelom Cellometer). (b). Percentage of neutrophils determined using FACS staining with FITC Ly6g antibody analyzed with FlowJo. (c) Total number of neutrophils calculated by multiplying total cells number by neutrophils percentage. (d) Bacteria enumeration from air pouch fluids using drop plate method and grown for 3 days in an aerobic chamber.

(A)

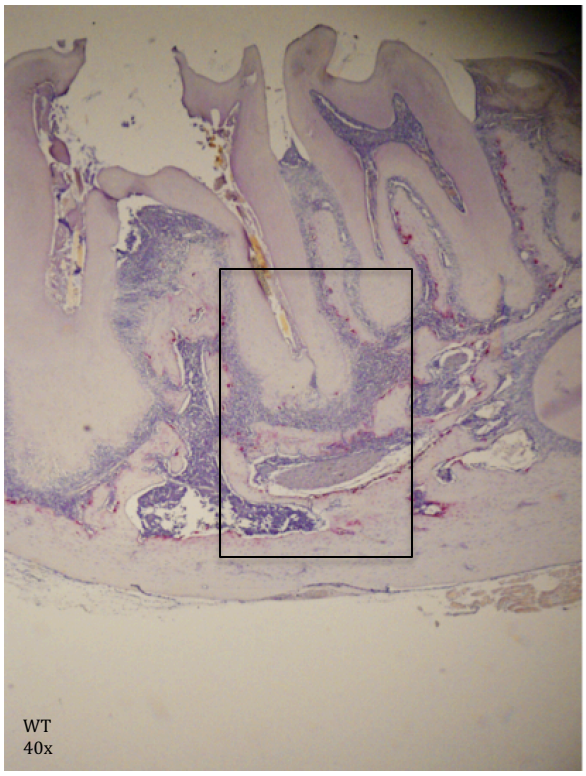

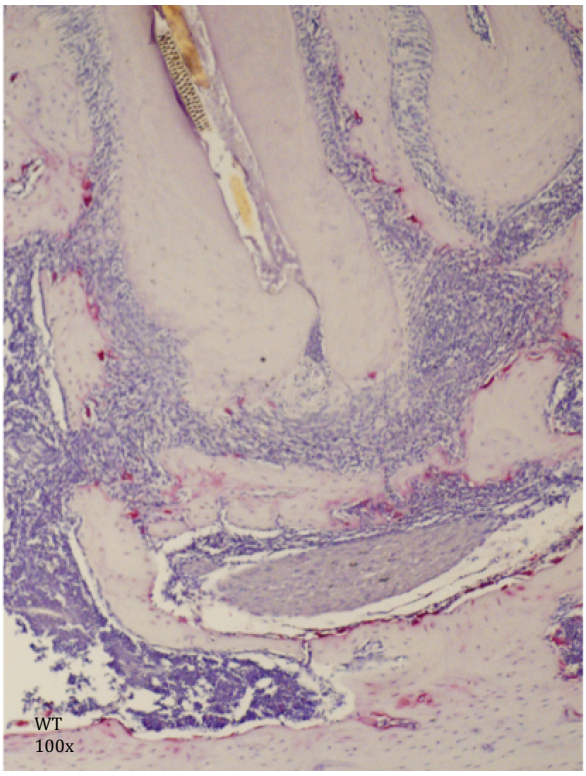

(B)

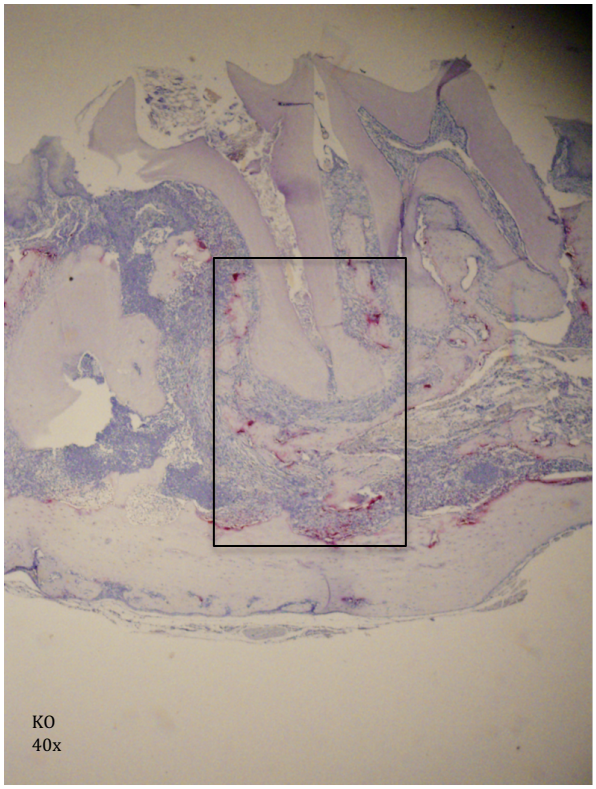

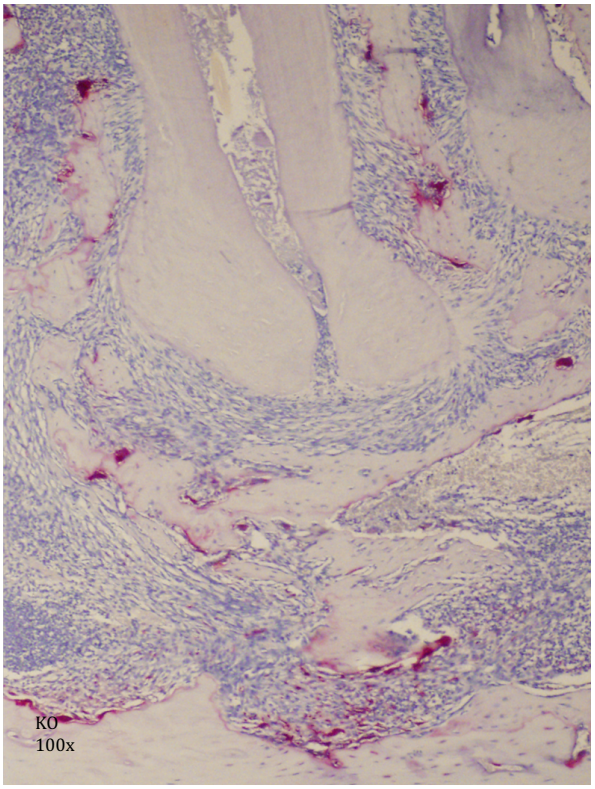

(C)

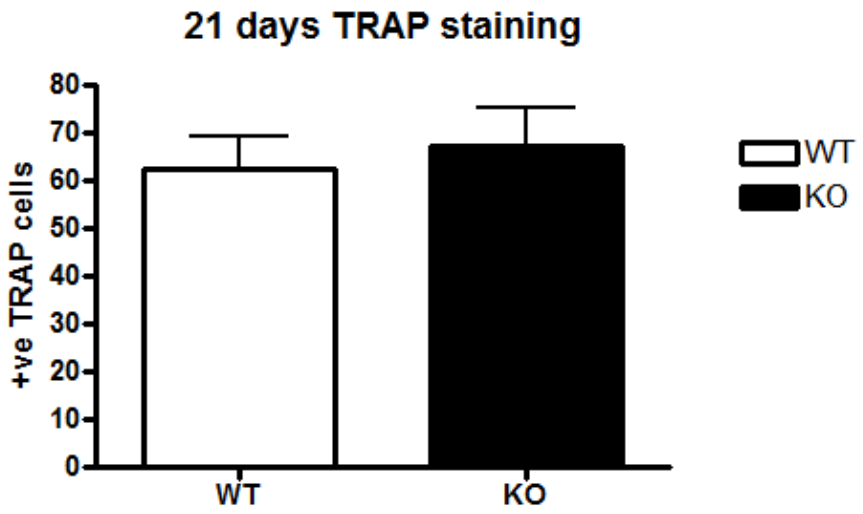

Figure 12. TRAP staining of 21days after infection. (a) Images of 21 days WT showing positive TRAP cells. (b) Images of 21 days KO showing positive TRAP cells. (c) TRAP staining did not show a difference in osteoclast numbers between the αv-tie2cre experimental and WT control groups in 21 days samples measured from one field using 40x magnification picture.

(A)

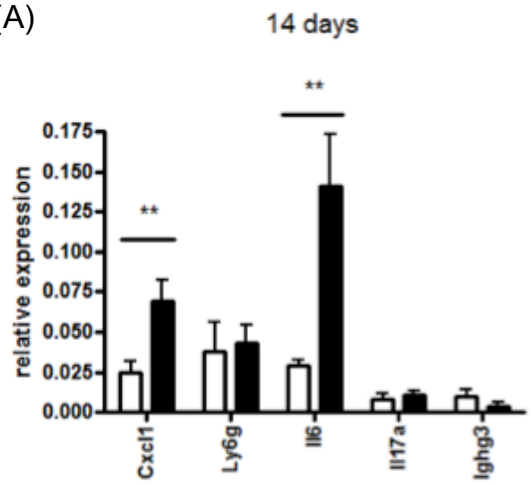
14 days
relative expression
0.175
0.150
0.125
0.100
0.075
0.050
0.025
0.000
**
**
Cxcl1
Ly6g
Il6
Il17a
Ighg3
WT
KO

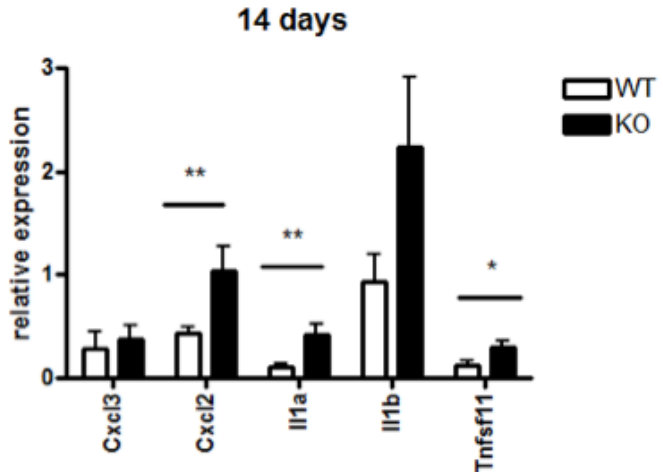
14 days
relative expression
3
2
1
0
**
**
*
Cxcl3
Cxcl2
Il1a
Il1b
Tnfsf11
WT
KO

(B)

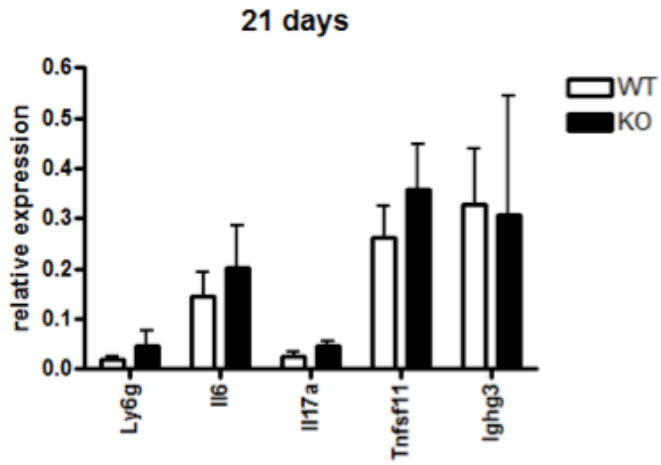
21 days
relative expression
0.6
0.5
0.4
0.3
0.2
0.1
0.0
Ly6g
Il6
Il17a
Tnfsf11
Ighg3
WT
KO

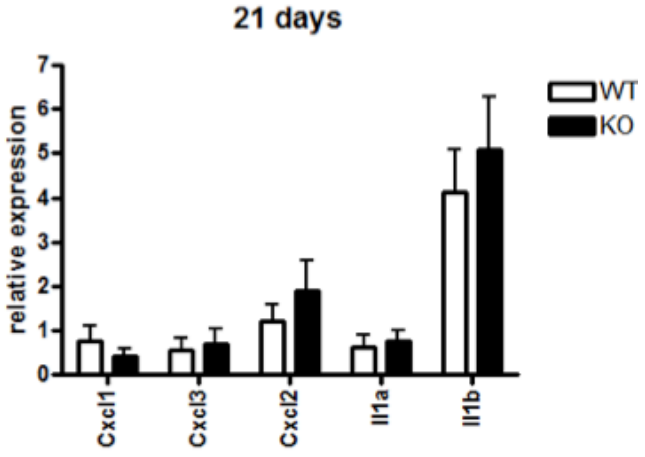
21 days
relative expression
7
6
5
4
3
2
1
0
Cxcl1
Cxcl3
Cxcl2
Il1a
Il1b
WT
KO

(C)

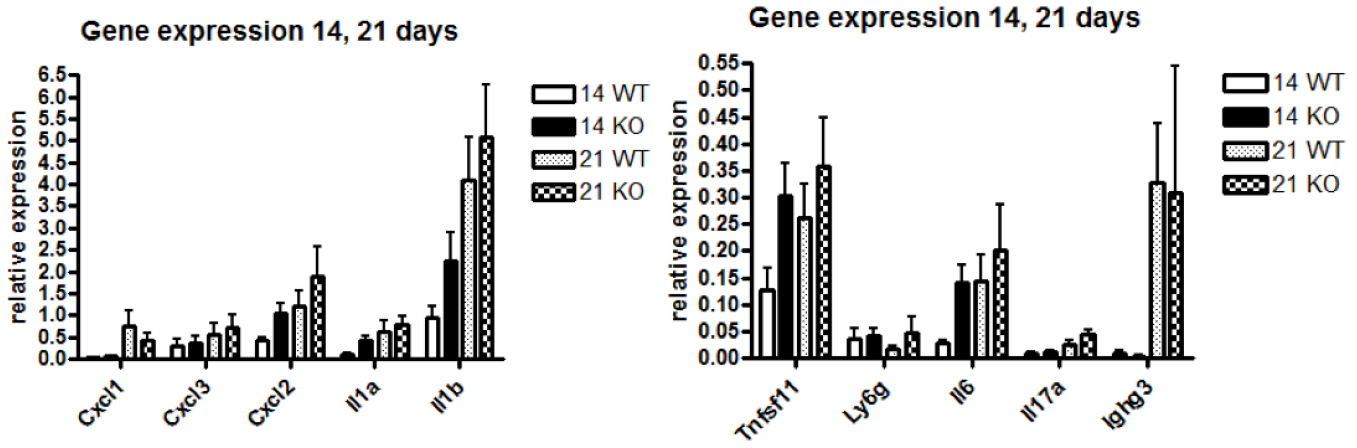

(D)

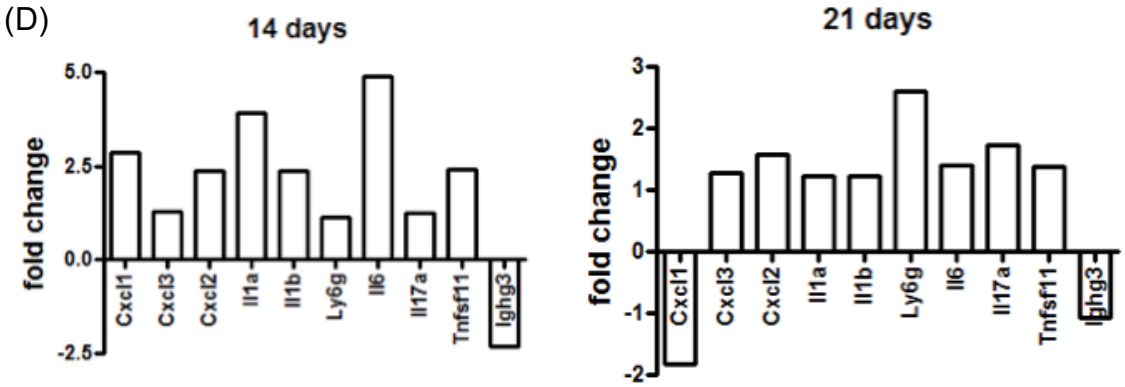

Figure 13. qPCR genes expression of av-tie2cre and WT relative to Dad1 as a reference gene. (a) 14 days after pulp exposure (n. WT=5, KO=7). (b) 21days after pulp exposure (n. WT=6, KO=7). (c) 14 and 21 days put together for gene expression changes between two time points. (d) Fold-change in 14 and 21 days samples in KO compared to WT. (* p-value <0.05, **<0.02).

Symbol	Description	Fold Change	p-value
LOC100862198	uncharacterized LOC100862198	20.7	0.000363783
LOC100862373	uncharacterized LOC100862373	18.1	0.031746361
Gm19767	predicted gene, 19767	17.1	0.001500366
Cxcl3	chemokine (C-X-C motif) ligand 3	13.1	0.034847292
Krt13	keratin 13	8.9	0.004602212
Krt17	keratin 17	6.1	0.038461764
LOC100862086	uncharacterized LOC100862086	5.7	0.007405421

Table 4. Microarray data, overexpressed genes that has more than 5 fold change increase in KO compared to WT and p-value<0.05.

Symbol	Description	Fold Change	p- value
Igkv15-103	immunoglobulin kappa chain variable 15-103	-5.2	0.046046531
Ighv1-58	immunoglobulin heavy variable 1-58	-5.9	0.000019759
Trbj1-1	T cell receptor beta joining 1-1	-6.3	0.022814065
Igkv1-110	immunoglobulin kappa variable 1-110	-7.1	0.01314995
Igkv3-2	immunoglobulin kappa variable 3-2	-11.2	0.035365782
Ighv11-1	immunoglobulin heavy variable 11-1	-12.3	0.011818555
Igkv4-91	immunoglobulin kappa chain variable 4-91	-15.6	0.002694496
Ighv1-81	immunoglobulin heavy variable 1-81	-17.2	0.002881718
Igkv9-120	immunoglobulin kappa chain variable 9-120	-18.6	0.036331523
Igkv19-93	immunoglobulin kappa chain variable 19-93	-21.1	0.004219346
Igkv4-80	immunoglobulin kappa variable 4-80	-22.6	0.00150687
Ighg3	Immunoglobulin heavy constant gamma 3	-23.3	0.005325556
Ighv11-2	immunoglobulin heavy variable V11-2	-25.5	0.000469288
Ighv4-1	immunoglobulin heavy variable 4-1	-27.5	0.002569031
Igkv8-24	immunoglobulin kappa chain variable 8-24	-30.4	0.008183208
Igkv1-133	immunoglobulin kappa variable 1-133	-44.6	0.007957113
Igkv1-135	immunoglobulin kappa variable 1-135	-45.7	0.001693435
Ighv1-12	immunoglobulin heavy variable V1-12	-49.3	0.004491107
Igkv6-13	immunoglobulin kappa variable 6-13	-55.6	0.001741069

Table 5. Microarray data, genes that has more than 5 fold change decrease in KO compared to WT and p-value<0.05.

(A)

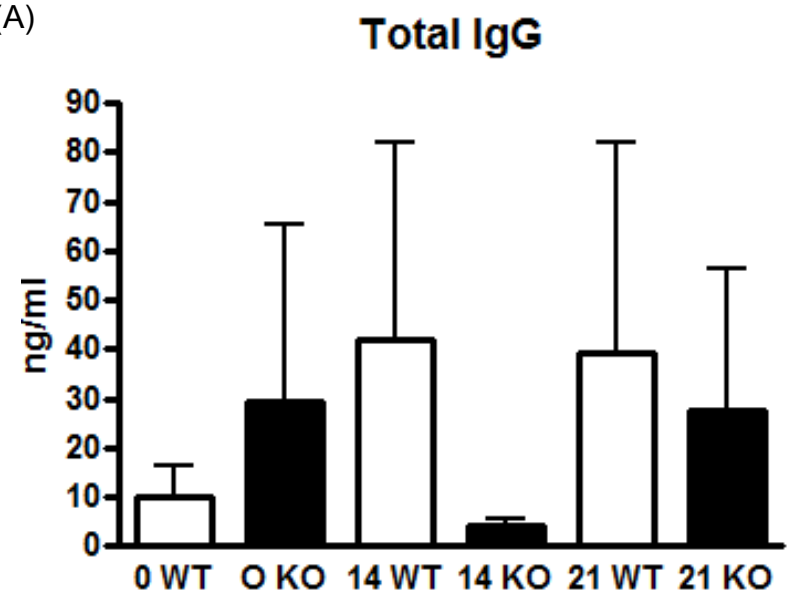

(B)

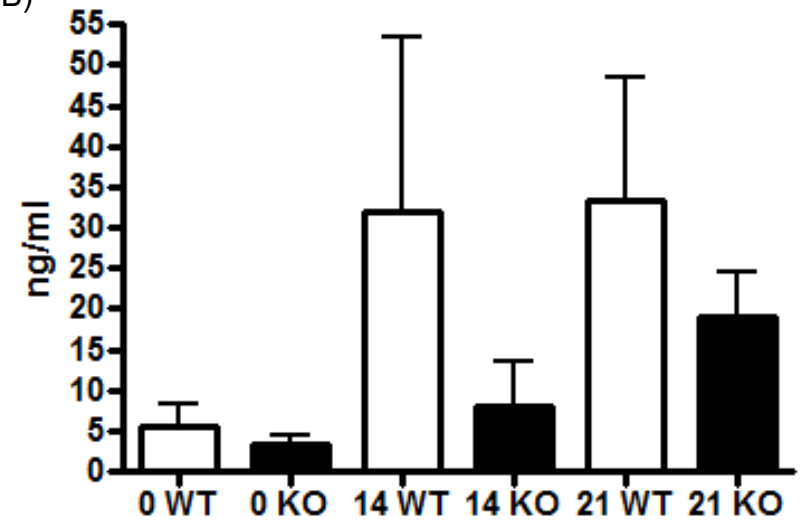

0 day: 6/group
14days: 4/group
21 days: 10/group

Figure 14. Blood plasma level measured using ELISA. (a) Total IgG in 0 day (control), 14 and 21 days in both av-tie2cre and WT. (b) IgG3 in 0 day (control), 14 and 21 days in both av-tie2cre and WT.

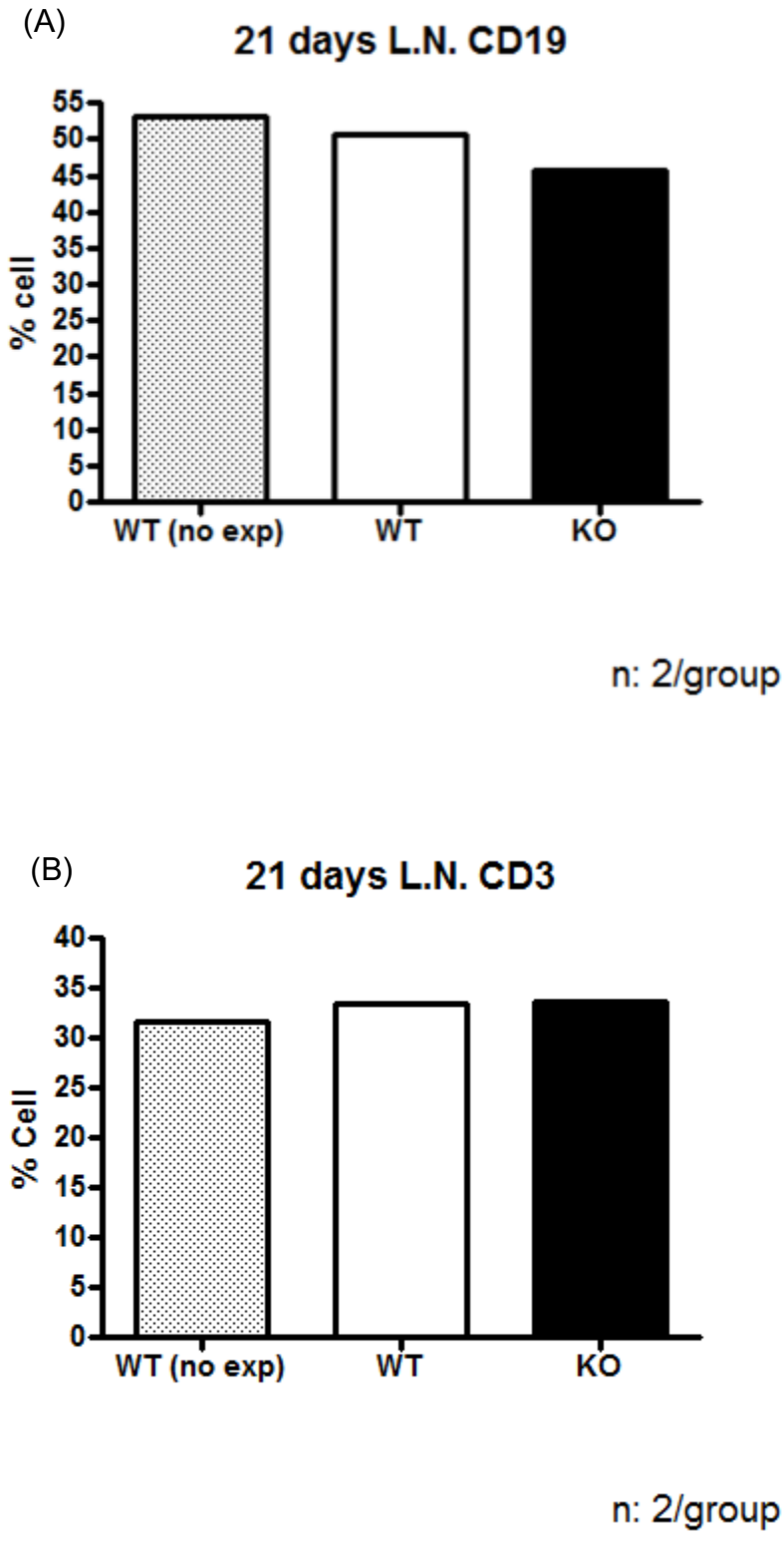

Figure 15. Mandibular lymph node analysis after 21 days pulp exposure. (a) B cell percentage in cervical lymph nodes in av-tie2cre and WT analyzed in FACS using CD19. (b) T cell percentage Mandibular lymph nodes in av-tie2cre and WT analyzed in FACS using CD3.

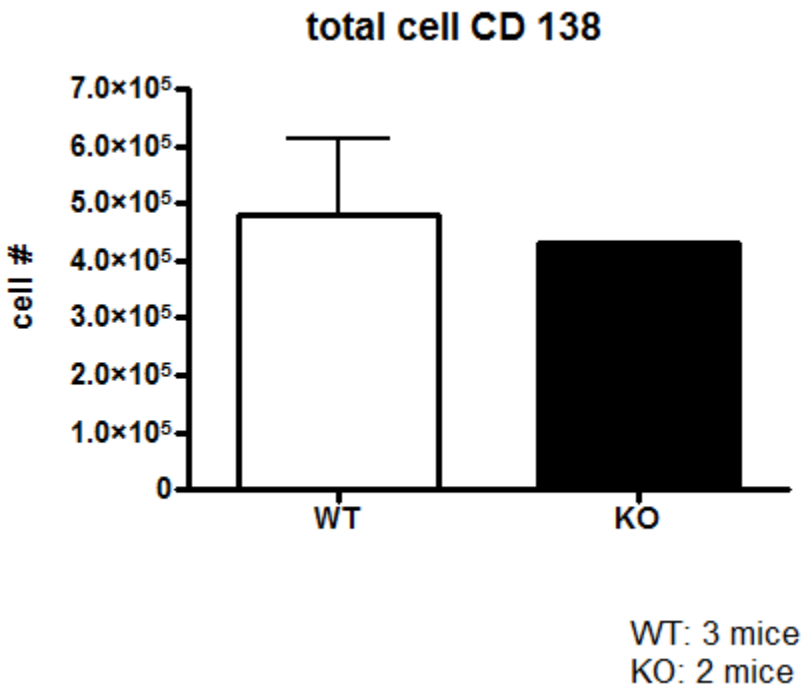

Figure 16. Air pouch fluids CD 138 plasma cells, percentage of plasma cells CD138 in cells collected from air pouch 24 hours after bacteria inoculation analyzed using FACS. In KO and WT.

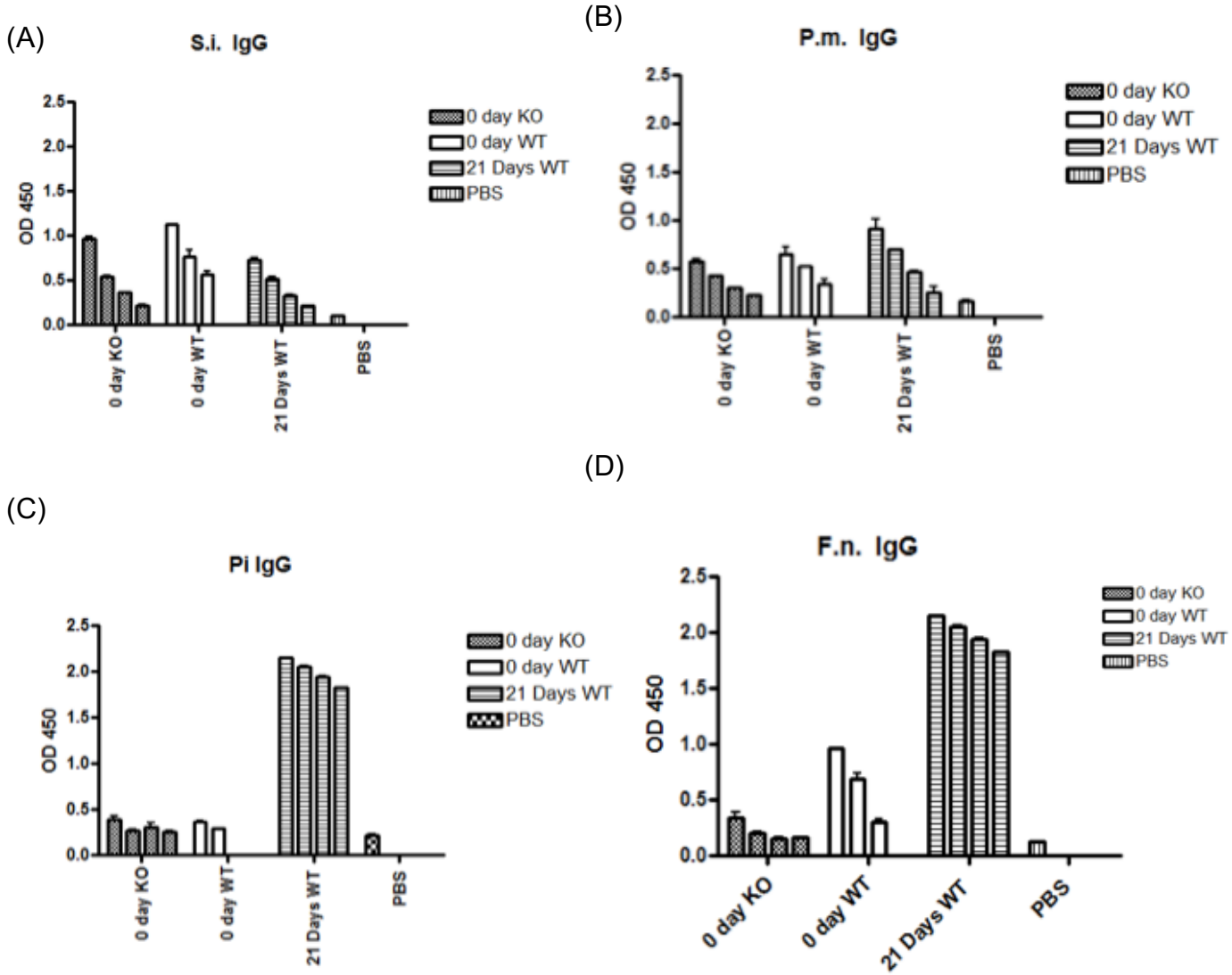

Figure 17. Bacteria specific IgG. Specific bacteria incubated with four dilutions of blood plasma (from left to right, 1/100, 1/200, 1/400, 1/800 of 0 day WT, KO and 21 days WT), measured with OD 450nm (a) *Streptococcus intermedius*, (b)*Parvimonas micra*, (c)*Prevotella intermedia*, (d) *Fusobacterium nucleatum*.

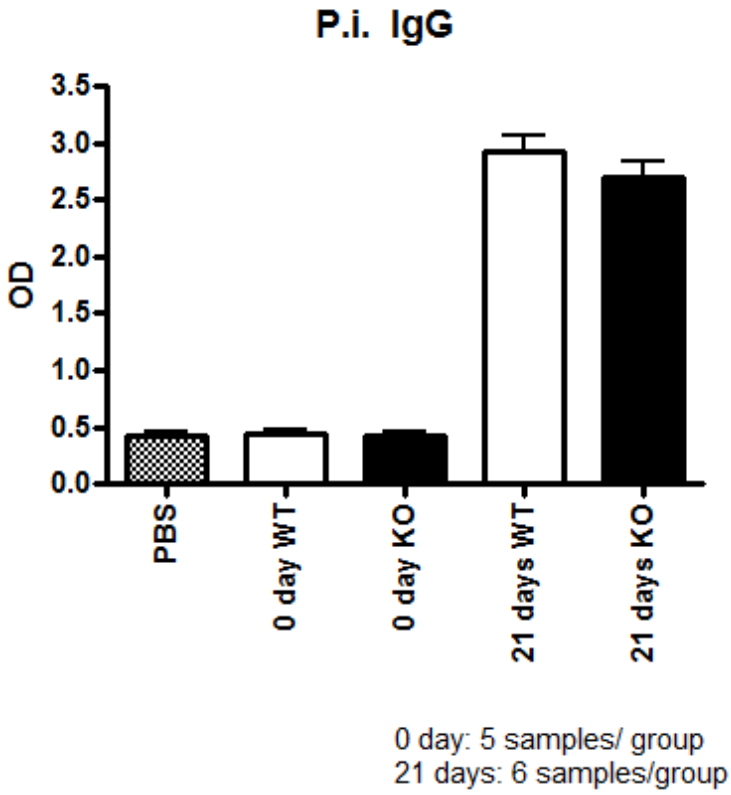

Figure 18. Bacteria specific IgG. *Prevotella intermedia* incubated with 1/400 dilutions of 21days blood plasma WT and KO, measured with OD 450nm.

Reference:

1. Kakehashi S, Stanley HR, Fitzgerald RJ. The Effects of Surgical Exposures of Dental Pulps in Germ-Free and Conventional Laboratory Rats. Oral surgery, oral medicine, and oral pathology 1965;20:340-349.
2. Moller AJ, Fabricius L, Dahlen G, Ohman AE, Heyden G. Influence on periapical tissues of indigenous oral bacteria and necrotic pulp tissue in monkeys. Scandinavian journal of dental research 1981;89(6):475-484.
3. Nair PN. Apical periodontitis: a dynamic encounter between root canal infection and host response. Periodontology 2000 1997;13:121-148.
4. Nair PN. Pathogenesis of apical periodontitis and the causes of endodontic failures. Critical reviews in oral biology and medicine : an official publication of the American Association of Oral Biologists 2004;15(6):348-381.
5. Siqueira JF, Jr., Rocas IN. Diversity of endodontic microbiota revisited. Journal of dental research 2009;88(11):969-981.
6. Siqueira JF. Endodontic infections: Concepts, paradigms, and perspectives. Oral Surgery, Oral Medicine, Oral Pathology, Oral Radiology, and Endodontology 2002;94(3):281-293.
7. Sundqvist G. Associations between microbial species in dental root canal infections. Oral microbiology and immunology 1992;7(5):257-262.
8. Gaudin A, Renard E, Hill M, Bouchet-Delbos L, Bienvenu-Louvet G, Farges JC, et al. Phenotypic analysis of immunocompetent cells in healthy human dental pulp. Journal of endodontics 2015;41(5):621-627.
9. Jontell M, Gunraj MN, Bergenholtz G. Immunocompetent cells in the normal dental pulp. Journal of dental research 1987;66(6):1149-1153.
10. Bergenholtz G, Lindhe J. Effect of soluble plaque factors on inflammatory reactions in the dental pulp. Scandinavian journal of dental research 1975;83(3):153-158.
11. Bergenholtz G. Iatrogenic injury to the pulp in dental procedures: aspects of pathogenesis, management and preventive measures. International dental journal 1991;41(2):99-110.
12. Yamasaki M, Kumazawa M, Kohsaka T, Nakamura H, Kameyama Y. Pulpal and periapical tissue reactions after experimental pulpal exposure in rats. Journal of endodontics 1994;20(1):13-17.
13. Kawashima N, Okiji T, Kosaka T, Suda H. Kinetics of macrophages and lymphoid cells during the development of experimentally induced periapical lesions in rat molars: a quantitative immunohistochemical study. Journal of endodontics 1996;22(6):311-316.
14. Stashenko P. Role of immune cytokines in the pathogenesis of periapical lesions. Endodontics & dental traumatology 1990;6(3):89-96.
15. Stern MH, Dreizen S, Mackler BF, Selbst AG, Levy BM. Quantitative analysis of cellular composition of human periapical granuloma. Journal of endodontics 1981;7(3):117-122.

16. Kopp W, Schwarting R. Differentiation of T lymphocyte subpopulations, macrophages, and HLA-DR-restricted cells of apical granulation tissue. Journal of endodontics 1989;15(2):72-75.
17. Stashenko P, Yu SM. T helper and T suppressor cell reversal during the development of induced rat periapical lesions. Journal of dental research 1989;68(5):830-834.
18. Langeland K, Block RM, Grossman LI. A histopathologic and histobacteriologic study of 35 periapical endodontic surgical specimens. Journal of endodontics 1977;3(1):8-23.
19. Yu SM, Stashenko P. Identification of inflammatory cells in developing rat periapical lesions. Journal of endodontics 1987;13(11):535-540.
20. Wang CY, Stashenko P. Characterization of bone-resorbing activity in human periapical lesions. Journal of endodontics 1993;19(3):107-111.
21. Kawashima N, Suzuki N, Yang G, Ohi C, Okuhara S, Nakano-Kawanishi H, et al. Kinetics of RANKL, RANK and OPG expressions in experimentally induced rat periapical lesions. Oral surgery, oral medicine, oral pathology, oral radiology, and endodontics 2007;103(5):707-711.
22. Balto K, Sasaki H, Stashenko P. Interleukin-6 deficiency increases inflammatory bone destruction. Infection and immunity 2001;69(2):744-750.
23. Hou L, Sasaki H, Stashenko P. Toll-like receptor 4-deficient mice have reduced bone destruction following mixed anaerobic infection. Infection and immunity 2000;68(8):4681-4687.
24. Sasaki H, Suzuki N, Kent R, Jr., Kawashima N, Takeda J, Stashenko P. T cell response mediated by myeloid cell-derived IL-12 is responsible for Porphyromonas gingivalis-induced periodontitis in IL-10-deficient mice. Journal of immunology (Baltimore, Md. : 1950) 2008;180(9):6193-6198.
25. Van Dyke TE, Taubman MA, Ebersole JL, Haffajee AD, Socransky SS, Smith DJ, et al. The Papillon-Lefevre syndrome: neutrophil dysfunction with severe periodontal disease. Clinical immunology and immunopathology 1984;31(3):419-429.
26. Cohen JS, Reader A, Fertel R, Beck M, Meyers WJ. A radioimmunoassay determination of the concentrations of prostaglandins E2 and F2alpha in painful and asymptomatic human dental pulps. Journal of endodontics 1985;11(8):330-335.
27. Bowen TJ, Ochs HD, Altman LC, Price TH, Van Epps DE, Brautigan DL, et al. Severe recurrent bacterial infections associated with defective adherence and chemotaxis in two patients with neutrophils deficient in a cell-associated glycoprotein. The Journal of pediatrics 1982;101(6):932-940.
28. Schenkein HA, Van Dyke TE. Early-onset periodontitis: systemic aspects of etiology and pathogenesis. Periodontology 2000 1994;6:7-25.
29. Kawashima N, Niederman R, Hynes RO, Ullmann-Cullere M, Stashenko P. Infection-stimulated infraosseus inflammation and bone destruction is increased in P-/E-selectin knockout mice. Immunology 1999;97(1):117-123.
30. Kawashima N OT, Kosaka T, Suda H. Effects of cyclophosphamide on the development of experimentally-induced periapical lesions in the rat. Jpn j Conserv Dent 1993;36:1388-1396.

31. Yamasaki M, Kumazawa M, Kohsaka T, Nakamura H. Effect of methotrexate-induced neutropenia on rat periapical lesion. Oral surgery, oral medicine, and oral pathology 1994;77(6):655-661.
32. Stashenko P, Wang CY, Riley E, Wu Y, Ostroff G, Niederman R. Reduction of infection-stimulated periapical bone resorption by the biological response modifier PGG glucan. Journal of dental research 1995;74(1):323-330.
33. Torabinejad M, Kettering JD. Identification and relative concentration of B and T lymphocytes in human chronic periapical lesions. Journal of endodontics 1985;11(3):122-125.
34. Stoufi ED, Taubman MA, Ebersole JL, Smith DJ, Stashenko PP. Phenotypic analyses of mononuclear cells recovered from healthy and diseased human periodontal tissues. Journal of clinical immunology 1987;7(3):235-245.
35. Pulver WH, Taubman MA, Smith DJ. Immune components in human dental periapical lesions. Archives of oral biology 1978;23(6):435-443.
36. Matthews JB, Mason GI. Immunoglobulin producing cells in human periapical granulomas. The British journal of oral surgery 1983;21(3):192-197.
37. Stashenko P, Yu SM, Wang CY. Kinetics of immune cell and bone resorptive responses to endodontic infections. Journal of endodontics 1992;18(9):422-426.
38. Teles R, Wang CY, Stashenko P. Increased susceptibility of RAG-2 SCID mice to dissemination of endodontic infections. Infect Immun 1997;65(9):3781-3787.
39. Hou L, Sasakj H, Stashenko P. B-Cell deficiency predisposes mice to disseminating anaerobic infections: protection by passive antibody transfer. Infect Immun 2000;68(10):5645-5651.
40. Cua DJ, Tato CM. Innate IL-17-producing cells: the sentinels of the immune system. Nature reviews. Immunology 2010;10(7):479-489.
41. AlShwaimi E, Berggreen E, Furusho H, Rossall JC, Dobeck J, Yoganathan S, et al. IL-17 receptor A signaling is protective in infection-stimulated periapical bone destruction. Journal of immunology (Baltimore, Md. : 1950) 2013;191(4):1785-1791.
42. Shen F, Ruddy MJ, Plamondon P, Gaffen SL. Cytokines link osteoblasts and inflammation: microarray analysis of interleukin-17- and TNF-alpha-induced genes in bone cells. Journal of leukocyte biology 2005;77(3):388-399.
43. Weber GF, Ashkar S, Glimcher MJ, Cantor H. Receptor-ligand interaction between CD44 and osteopontin (Eta-1). Science (New York, N.Y.) 1996;271(5248):509-512.
44. Zhu B, Suzuki K, Goldberg HA, Rittling SR, Denhardt DT, McCulloch CA, et al. Osteopontin modulates CD44-dependent chemotaxis of peritoneal macrophages through G-protein-coupled receptors: evidence of a role for an intracellular form of osteopontin. Journal of cellular physiology 2004;198(1):155-167.
45. Koguchi Y, Kawakami K, Kon S, Segawa T, Maeda M, Uede T, et al. Penicillium marneffei causes osteopontin-mediated production of interleukin-12 by peripheral blood mononuclear cells. Infection and immunity 2002;70(3):1042-1048.
46. Rittling SR, Zetterberg C, Yagiz K, Skinner S, Suzuki N, Fujimura A, et al. Protective role of osteopontin in endodontic infection. Immunology 2010;129(1):105-114.

47. Wang KX, Denhardt DT. Osteopontin: role in immune regulation and stress responses. Cytokine & growth factor reviews 2008;19(5-6):333-345.
48. Koh A, da Silva AP, Bansal AK, Bansal M, Sun C, Lee H, et al. Role of osteopontin in neutrophil function. Immunology 2007;122(4):466-475.
49. Inoue M, Shinohara ML. Cutting edge: Role of osteopontin and integrin alphav in T cell-mediated anti-inflammatory responses in endotoxemia. Journal of immunology (Baltimore, Md. : 1950) 2015;194(12):5595-5598.
50. Hu DD, Lin EC, Kovach NL, Hoyer JR, Smith JW. A biochemical characterization of the binding of osteopontin to integrins alpha v beta 1 and alpha v beta 5. J Biol Chem 1995;270(44):26232-26238.
51. Hynes RO. Integrins: bidirectional, allosteric signaling machines. Cell 2002;110(6):673-687.
52. Shattil SJ, Kim C, Ginsberg MH. The final steps of integrin activation: the end game. Nature reviews. Molecular cell biology 2010;11(4):288-300.
53. Calderwood DA. Integrin activation. Journal of cell science 2004;117(Pt 5):657-666.
54. Garcia AJ. Get a grip: integrins in cell-biomaterial interactions. Biomaterials 2005;26(36):7525-7529.
55. Bader BL, Rayburn H, Crowley D, Hynes RO. Extensive vasculogenesis, angiogenesis, and organogenesis precede lethality in mice lacking all alpha v integrins. Cell 1998;95(4):507-519.
56. Lacy-Hulbert A, Smith AM, Tissire H, Barry M, Crowley D, Bronson RT, et al. Ulcerative colitis and autoimmunity induced by loss of myeloid alphav integrins. Proceedings of the National Academy of Sciences of the United States of America 2007;104(40):15823-15828.
57. Felding-Habermann B, Cheresh DA. Vitronectin and its receptors. Current opinion in cell biology 1993;5(5):864-868.
58. Venstrom K, Reichardt L. Beta 8 integrins mediate interactions of chick sensory neurons with laminin-1, collagen IV, and fibronectin. Molecular biology of the cell 1995;6(4):419-431.
59. Munger JS, Huang X, Kawakatsu H, Griffiths MJ, Dalton SL, Wu J, et al. The integrin alpha v beta 6 binds and activates latent TGF beta 1: a mechanism for regulating pulmonary inflammation and fibrosis. Cell 1999;96(3):319-328.
60. Travis MA, Reizis B, Melton AC, Masteller E, Tang Q, Proctor JM, et al. Loss of integrin alpha(v)beta8 on dendritic cells causes autoimmunity and colitis in mice. Nature 2007;449(7160):361-365.
61. Savill J, Dransfield I, Hogg N, Haslett C. Vitronectin receptor-mediated phagocytosis of cells undergoing apoptosis. Nature 1990;343(6254):170-173.
62. Albert ML, Pearce SF, Francisco LM, Sauter B, Roy P, Silverstein RL, et al. Immature dendritic cells phagocytose apoptotic cells via alphavbeta5 and CD36, and cross-present antigens to cytotoxic T lymphocytes. The Journal of experimental medicine 1998;188(7):1359-1368.

63. Rubartelli A, Poggi A, Zocchi MR. The selective engulfment of apoptotic bodies by dendritic cells is mediated by the alpha(v)beta3 integrin and requires intracellular and extracellular calcium. European journal of immunology 1997;27(8):1893-1900.
64. Savill J, Dransfield I, Gregory C, Haslett C. A blast from the past: clearance of apoptotic cells regulates immune responses. Nature reviews. Immunology 2002;2(12):965-975.
65. Acharya M, Mukhopadhyay S, Paidassi H, Jamil T, Chow C, Kissler S, et al. alphav Integrin expression by DCs is required for Th17 cell differentiation and development of experimental autoimmune encephalomyelitis in mice. The Journal of clinical investigation 2010;120(12):4445-4452.
66. Gorelik L, Flavell RA. Abrogation of TGFbeta signaling in T cells leads to spontaneous T cell differentiation and autoimmune disease. Immunity 2000;12(2):171-181.
67. Taipale J, Saharinen J, Keski-Oja J. Extracellular matrix-associated transforming growth factor-beta: role in cancer cell growth and invasion. Advances in cancer research 1998;75:87-134.
68. Joyce ME, Roberts AB, Sporn MB, Bolander ME. Transforming growth factor-beta and the initiation of chondrogenesis and osteogenesis in the rat femur. The Journal of cell biology 1990;110(6):2195-2207.
69. Chan LT, Zhong S, Naqvi AR, Self-Fordham J, Nares S, Bair E, et al. MicroRNAs: new insights into the pathogenesis of endodontic periapical disease. Journal of endodontics 2013;39(12):1498-1503.
70. Lin SK, Hong CY, Chang HH, Chiang CP, Chen CS, Jeng JH, et al. Immunolocalization of macrophages and transforming growth factor-beta 1 in induced rat periapical lesions. Journal of endodontics 2000;26(6):335-340.
71. Ng YL, Mann V, Gulabivala K. A prospective study of the factors affecting outcomes of nonsurgical root canal treatment: part 1: periapical health. International endodontic journal 2011;44(7):583-609.
72. Van Dyke TE. Control of inflammation and periodontitis. Periodontology 2000 2007;45:158-166.
73. Cainzos M. Review of the guidelines for complicated skin and soft tissue infections and intra-abdominal infections--are they applicable today? Clinical microbiology and infection : the official publication of the European Society of Clinical Microbiology and Infectious Diseases 2008;14 Suppl 6:9-18.
74. Sasaki H, Hou L, Belani A, Wang CY, Uchiyama T, Muller R, et al. IL-10, but not IL-4, suppresses infection-stimulated bone resorption in vivo. J Immunol 2000;165(7):3626-3630.
75. Kisanuki YY, Hammer RE, Miyazaki J, Williams SC, Richardson JA, Yanagisawa M. Tie2-Cre transgenic mice: a new model for endothelial cell-lineage analysis in vivo. Dev. Biol. 2001;230(2):230-242.
76. Overstreet MG, Gaylo A, Angermann BR, Hughson A, Hyun YM, Lambert K, et al. Inflammation-induced interstitial migration of effector CD4(+) T cells is dependent on integrin alphaV. Nature immunology 2013;14(9):949-958.

77. Nau GJ, Liaw L, Chupp GL, Berman JS, Hogan BL, Young RA. Attenuated host resistance against Mycobacterium bovis BCG infection in mice lacking osteopontin. Infection and immunity 1999;67(8):4223-4230.
78. Heilmann K, Hoffmann U, Witte E, Loddenkemper C, Sina C, Schreiber S, et al. Osteopontin as two-sided mediator of intestinal inflammation. Journal of cellular and molecular medicine 2009;13(6):1162-1174.
79. Berton G, Lowell CA. Integrin signalling in neutrophils and macrophages. Cellular signalling 1999;11(9):621-635.
80. Yokosaki Y, Matsuura N, Sasaki T, Murakami I, Schneider H, Higashiyama S, et al. The integrin alpha(9)beta(1) binds to a novel recognition sequence (SVVYGLR) in the thrombin-cleaved amino-terminal fragment of osteopontin. The Journal of biological chemistry 1999;274(51):36328-36334.
81. Taooka Y, Chen J, Yednock T, Sheppard D. The integrin alpha9beta1 mediates adhesion to activated endothelial cells and transendothelial neutrophil migration through interaction with vascular cell adhesion molecule-1. The Journal of cell biology 1999;145(2):413-420.
82. Alshwaimi E, Purcell P, Kawai T, Sasaki H, Oukka M, Campos-Neto A, et al. Regulatory T cells in mouse periapical lesions. Journal of endodontics 2009;35(9):1229-1233.
83. Witowski J, Pawlaczyk K, Breborowicz A, Scheuren A, Kuzlan-Pawlaczyk M, Wisniewska J, et al. IL-17 stimulates intraperitoneal neutrophil infiltration through the release of GRO alpha chemokine from mesothelial cells. Journal of immunology (Baltimore, Md. : 1950) 2000;165(10):5814-5821.
84. Wykes M, Pombo A, Jenkins C, MacPherson GG. Dendritic cells interact directly with naive B lymphocytes to transfer antigen and initiate class switching in a primary T-dependent response. Journal of immunology (Baltimore, Md. : 1950) 1998;161(3):1313-1319.